EL SEVIER

Contents lists available at ScienceDirect

# Science of the Total Environment

journal homepage: www.elsevier.com/locate/scitotenv



# Isotopic and element ratios fingerprint salinization impact from beneficial use of oil and gas produced water in the Western U.S.



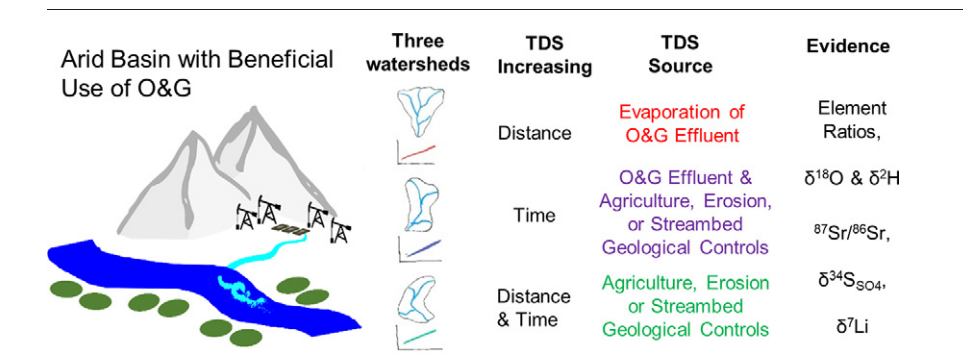
Bonnie McDevitt <sup>a</sup>, Molly C. McLaughlin <sup>b</sup>, David S. Vinson <sup>c</sup>, Thomas J. Geeza <sup>a,d</sup>, Jens Blotevogel <sup>b</sup>, Thomas Borch <sup>b,e,f</sup>, Nathaniel R. Warner <sup>a,\*</sup>

- <sup>a</sup> Department of Civil and Environmental Engineering, The Pennsylvania State University, United States of America
- b Department of Civil and Environmental Engineering, Colorado State University, United States of America
- <sup>c</sup> Department of Geography and Earth Sciences, University of North Carolina at Charlotte, United States of America
- <sup>d</sup> EES-14, Los Alamos National Laboratory, Los Alamos, NM 87544, United States of America
- <sup>e</sup> Department of Chemistry, Colorado State University, United States of America
- f Department of Soil and Crop Sciences, Colorado State University, United States of America

#### HIGHLIGHTS

- NPDES permits allow treated 0&G produced water to be discharged for beneficial use
- Elevated TDS is driven by sulfate, sodium and calcium.
- Cl-normalized ratios and  $\delta^2H$  and  $\delta^{18}O$  of water provided evidence of evaporation.
- $^{87}$ Sr/ $^{86}$ Sr and  $\delta^{34}$ S<sub>SO4</sub> determined TDS increases derived from a non-O&G source.
- <sup>3</sup>Li was useful to distinguish NPDES discharges from river and background water.

# GRAPHICAL ABSTRACT



# ARTICLE INFO

Article history: Received 11 October 2019 Received in revised form 16 January 2020 Accepted 28 January 2020 Available online 31 January 2020

Editor: Yolanda Picó

Keywords: Evaporation Agriculture TDS Strontium Sulfate Lithium

# ABSTRACT

Salinization of global freshwater resources is a concerning health and economic issue of the 21st century and requires serious management and study to understand how, and by what mechanism, Total Dissolved Solids (TDS) is changing in major watersheds. Oil and gas (0&G) produced water is a complex and saline (10-300 g/L TDS) wastewater often disposed to surface waters post-treatment. However, in western U.S. states, beneficial use of minimally treated O&G produced water discharged to ephemeral streams is permitted through the USEPA National Pollutant Discharge Elimination System (NPDES) for agriculture and wildlife propagation. In a remote Wyoming study region, beneficial use of O&G NPDES effluents annually contributes 13 billion L of water to surface water resources. The primary O&G TDS constituents are sulfate and sodium followed by chloride and calcium. Significant TDS increases from 2013 to 2016 in a large perennial river (River C) impacted by O&G effluent disposal, slight TDS increases in a perennial river (River B) and chronically elevated TDS (upwards of 2500 mg/L) in a smaller tributary (Tributary A) comprised mainly of O&G effluents led to an investigation of O&G impacts to surface waters in the region. Chloride-normalized metal ratios such as Br/Cl and  $\delta^2$ H and  $\delta^{18}$ O distinguished evaporation as the mechanism for increasing TDS derived from O&G on Tributary A, which is causing O&G effluents that meet NPDES regulations to not only exceed outfall regulations downstream where it is beneficially used for irrigation and drinking water but also exceed aquatic life and livestock recommended limits. <sup>87</sup>Sr/<sup>86</sup>Sr and  $\delta^{34}$ S<sub>SO4</sub> suggested minor impacts from O&G TDS loading on River C but also support an additional salinity source,

<sup>\*</sup> Corresponding author. E-mail address: nrw6@psu.edu (N.R. Warner).

such as streambed geological controls, the cause of significantly increasing TDS. While lithium isotopes provided insight into the O&G effluent origin ( $\delta^7$ Li ranged 9–10‰) and water-sediment interactions along O&G effluent streams, they did not function as distinct salinity tracers in the larger downstream rivers. This study suggests a multi-isotope ( $^{87}$ Sr/ $^{86}$ Sr and  $\delta^{34}$ SsO4) approach is often necessary for fingerprinting salinization sources and determining best management practices because multiple salinity sources and environmental mechanisms may need to be identified to protect water quality.

© 2020 Elsevier B.V. All rights reserved.

### 1. Introduction

Salinization of freshwater threatens human and ecological health, agricultural yields, economics of energy production, and drinking water security on a global scale. Salinization refers to the increase in Total Dissolved Solids (TDS) in water associated with increasing inorganic ion concentrations, Salinization of surface water can be a natural phenomenon where salts sourced from the weathering of aguifer minerals or dissolution of evaporites are leached from the unsaturated zone of soils into shallow groundwater or ephemeral streams. However, in many cases, anthropogenic point sources (i.e. oil and gas (O&G) produced water discharges, wastewater treatment facility outfalls) and non-point sources (i.e. agricultural return flows, road deicing) enhance the extent and speed of natural salinization processes (Vengosh, 2013). Kaushal et al. (2018a, 2018b) noted the continental scale of the "salinization syndrome" in coordination with the less discussed alkalinization of surface waters - the primary causes of increasing salinity being agriculture, road deicing, resource extraction and land clearing (Cañedo-Argüelles et al., 2013; Kaushal et al., 2018a, 2018b; Williams, 2001).

Clearing of land can disturb native soils and increase natural weathering rates leading to increased alkalinity in streams from increased carbonate dissolution or ion exchange processes (Vengosh, 2013). Annually applying tens of thousands of metric tons of road salt as well as commercial and O&G brines for dust suppression and deicing have led to chloride concentration increases in Midwestern and Northeastern U.S. metropolitan areas (Kaushal et al., 2018b). In these regions baseline chloride concentrations are frequently greater than the maximum recommended chronic exposure limit for the protection of freshwater life of 230 mg/L and secondary U.S. Environmental Protection Agency (EPA) drinking water standard of 250 mg/L (Corsi et al., 2015; Dugan et al., 2017; Kelly et al., 2005; Tasker et al., 2018). Chloride concentrations greater than this recommended limit for aquatic life were observed to cause aquatic plant mortality and inhibit reproduction, as well as facilitate establishment of invasive and halotolerant species leading to loss of biodiversity (James et al., 2009). The EPA and Wyoming secondary standard for TDS in drinking water is 500 mg/L, with a recommended safe limit of 500 to 2000 mg/L for agricultural use, and <2500 mg/L for livestock drinking water (Pick, 2011). Freshwater fish populations typically survive in TDS concentrations <1000 mg/L; however, lower TDS levels may be toxic to specific species depending on the concentrations of specific ions such as SO<sub>4</sub>, Cl, or Br (Raisbeck et al., 2008; Weber-Scannell and Duffy, 2007).

Wastewater disposal from both domestic and industrial sectors contributes salinity to receiving water bodies (Chetelat and Gaillardet, 2005; Daugherty et al., 2010; Vengosh et al., 2014; Warner et al., 2013a, 2013b). Corrosion of infrastructure linked to elevated salt concentrations among other factors not only has the potential to release lead and copper from pipes into drinking water but can also cause expensive pipe failure replacements (Kaushal, 2016; Stets et al., 2018).

O&G extraction in the United States generates 21 billion barrels (3.3 trillion L) of wastewater annually of which approximately 84% is reinjected into formations either for disposal or for enhanced oil recovery (EOR) processes (Clark and Veil, 2015). The remaining 16% is potentially discharged to freshwater receiving streams, evaporated and concentrated, while approximately 1% is beneficially used in semi-arid western states permitted through the National Pollutant Discharge

Elimination System (NPDES) under 40 CFR § 435 Subpart E for irrigation, livestock watering and wildlife propagation. Wyoming generates approximately 2.18 billion barrels (346 billion L) of produced water annually with approximately 600 O&G NPDES-permitted facilities under the beneficial use exemption (Clark and Veil, 2015; Guerra et al., 2011). In light of expected increases in produced water volumes, the EPA and U.S. Department of Energy (DOE) are currently seeking comments on a study regarding expansion of the beneficial use provision, which seeks alternatives to surface water disposal (EPA, 2018; Kondash et al., 2018).

Produced water chemistry varies as a function of geologic location and production history and is often a highly saline solution causing concern for drinking water intakes and aquatic life downstream (Blewett et al., 2017, 2018; Dresel and Rose, 2010; Geeza et al., 2018; McLaughlin et al., 2020a; Wilson and Vanbriesen, 2012). Sediment accumulation of radium associated with carbonate and sulfate precipitates downstream of O&G effluent surface water disposal act as a secondary salinity contaminant source under slight chemical equilibrium alterations (McDevitt et al., 2018; Van Sice et al., 2018). There are few studies on beneficial use of produced water in the western U.S., though use of coal bed methane and O&G produced water for irrigation, a major spill in the Williston Basin, and presence of persistent organic contaminants kilometers downstream of discharges have been reported (Bern et al., 2013; Cozzarelli et al., 2016; Lauer et al., 2016; McDevitt et al., 2018; McLaughlin et al., 2020b; Sedlacko et al., 2019).

Utilizing high salinity wastewater for irrigation in semi-arid regions can result in secondary salinization as a result of evaporation leaving behind residual salts in the soil, which inhibit the germination of plants and diminish growth and yields of crops (Hoffman et al., 1983). High sodium adsorption ratios (SAR), a measure of the concentration ratio of sodium ions to calcium and magnesium ions, are an observed issue in Wyoming produced waters, and can lead to deficiencies in crop potassium, magnesium and calcium due to sodium competition for plant root uptake (Bern et al., 2013). Likewise, high boron concentrations, associated with high salinity O&G produced water, are damaging to some crop species above 0.75 mg/L (Ayers and Wescot, 1994; Vengosh, 2013).

Salinity increases in a major river basin in Wyoming receiving discharge of minimally treated O&G produced water (referred to throughout as effluent) under NPDES beneficial use permitting were studied from 2013 to 2016. To understand the mechanism of salinization and to gauge potential environmental impacts anthropogenic salinity sources such as O&G effluent, agricultural return flows, evaporite dissolution, and cation exchange were investigated. Natural mechanisms such as stream flow, evaporation, and precipitation-dissolution of minerals were simultaneously monitored. Standard elemental geochemical techniques as described in other studies might fail to fingerprint a definitive salinity source and instead a combination of mechanisms and potential sources (Lgourna et al., 2014; Vinson et al., 2013; Warner et al., 2013b). This critical water management knowledge gap necessitates utilizing a regional multi-isotope approach (<sup>2</sup>H/<sup>1</sup>H,  $^{18}$ O/ $^{16}$ O,  $^{87}$ Sr/ $^{86}$ Sr,  $^{7}$ Li/ $^{6}$ Li,  $^{34}$ S/ $^{32}$ S) to fingerprint salinity and water sources as has been demonstrated in eastern U.S. studies related to O&G wastewater disposal (Chapman et al., 2012; Phan et al., 2016; Warner et al., 2014).

Strontium isotopes (87Sr/86Sr) are an excellent tracer of salinity sources as they do not significantly fractionate due to environmental

reactions, meaning co-occurring cation removal mechanisms such as cation exchange do not reduce their effectiveness. Strontium exhibits similar chemical and environmental behavior to calcium, which allows strontium isotopes to distinguish high sulfate concentrations derived from O&G discharges from native evaporite gypsum (CaSO<sub>4</sub>). Anthropogenic activities such as O&G extraction or agriculture can increase dissolution of gypsum from native soils, such as another Wyoming study concluded, although no isotopic analysis was performed (Bern et al., 2015). O&G discharges often have a narrow <sup>87</sup>Sr/<sup>86</sup>Sr range that is distinct compared to background river water allowing strontium isotopes to be used as an identifier of salinity sources, helping understand the origin of changes to downstream water chemistry (Chapman et al., 2012; Harkness et al., 2017; Warner et al., 2013a).

Lithium is released from clay mineral exchange sites due to fresh water injected into O&G formations as part of hydraulic fracturing or enhanced oil recovery processes (Barth, 1993; Macpherson et al., 2014; Warner et al., 2014). Because lithium concentrations are often elevated at NPDES facilities compared to surface waters, <sup>7</sup>Li/<sup>6</sup>Li ratios have potential to provide a strong tracer of O&G effluent contamination in downstream rivers. Lithium concentrations in O&G produced waters vary widely, up to >300 mg/L usually correlated with high chloride concentrations, while global river waters range from 1 to 50 µg/L (Macpherson et al., 2014; Phan et al., 2016; Warner et al., 2014). Global river water  $\delta^7$ Li generally ranges from 16 to 29% (Huh et al., 1998) while reported O&G conventional brines range from 10 to 25% and Marcellus brines from 6 to 10% (Phan et al., 2016; Warner et al., 2014). Lithium behaves differently than some other isotope systems in that the lighter <sup>6</sup>Li partitions into sediments, is incorporated into the structure or sorbed onto clay minerals and metal oxyhydroxides, and a small fractionation is associated with incorporation into mineral precipitates such as calcium carbonates leaving the aqueous phase enriched in <sup>7</sup>Li (Hindshaw et al., 2019; Marriott et al., 2004; Millot et al., 2010; Vigier et al., 2008). In our study area we expect the O&G effluent  $\delta^7$ Li at the discharge to not only be distinct from surface waters, but could also increase with distance downstream from the NPDES facility on the effluent stream due to removal of <sup>6</sup>Li by sorption and mineral precipitation. To the authors' knowledge, no comprehensive studies on lithium isotopes, concentrations, and transport behavior in rivers have been completed in the region.

Sulfur isotopes ( $^{34}$ S/ $^{32}$ S) are useful for determining the age of marine sulfur deposits. The two major mineral sources of S are pyrite in shales and organic rich sediments containing sulfate reducing bacteria, and gypsum deposits in limestones (Claypool et al., 1980). Dissolution of evaporites such as gypsum causes minimal fractionation of  $^{34}$ S/ $^{32}$ S so the ratio can be used to track the source of S (Porowski, 2014). For example, Tertiary deposits range in  $\delta^{34}$ S from +21 to +23% whereas Jurassic deposits range from +15 to +17% (Claypool et al., 1980). Sedimentary sulfate typically has a higher  $\delta^{34}$ S of +17% similar to the modern ocean of +20% whereas sedimentary sulfide has a lower  $\delta^{34}$ S of -18% (Sharp, 2007).

This study took place in a remote region of Wyoming that contains large O&G fields in upstream sagebrush drainage regions, utilized for cattle and wildlife rangelands, where O&G effluents are ultimately discharged downstream into two major perennial rivers (River B and River C) and a smaller tributary (Tributary A). Increasing TDS downstream of confluence points in the larger rivers caused concern and motivated synoptic sampling. The objective of this study is to determine the source of salinity increases in the three neighboring watersheds. This will be accomplished by (1) analyzing major and trace element ratios in O&G effluent, (2) investigating stable isotopes in water for evaporative effects on NPDES effluent streams and larger rivers, and (3) tracing sources of salinity utilizing <sup>87</sup>Sr/<sup>86</sup>Sr, <sup>7</sup>Li/<sup>6</sup>Li, and <sup>34</sup>S/<sup>32</sup>S ratios as contamination fingerprinting tools. The multi-isotope approach (Bouchaou et al., 2008; Lgourna et al., 2014; Szynkiewicz et al., 2012; Vengosh, 2013; Vinson et al., 2011; Warner et al., 2013c) can also potentially provide a proof of concept that isotopic tracers of O&G can be applied in semi-arid regions with multiple potential salinity sources such as agriculture, domestic wastewater, O&G, dissolution of local soils, and coexisting environmental mechanisms such as evaporation, chemical precipitation and dissolution, and ion exchange.

### 2. Materials and methods

# 2.1. Study site description & field sampling

Three neighboring Wyoming watersheds (A, B, C) were sampled at 30 GPS-located sites ten times from 2013 to 2016 in May and November 2013, May, July, and October 2014, July and October 2015, and June, August, and October 2016 (Fig. 1). Ten sites were sampled along the larger Tributary A (A1, A2, A3, A4), River B (B1, B2, B3) and River C (C1, C2, C3) with Sites A1, B1 and C1 reflecting a sample site upstream of the confluence between the O&G effluent streams and Tributary A, River B and River C, respectively. Seven O&G NPDES discharge effluents were sampled (DA-1, DA-2, DA-3, DB-1.0, DB-2.0, DB-4.0, DC-1) and are designated with a "D-." Three were located in watershed A and contributed to Tributary A (DA-1, DA-2, DA-3), three were in watershed B and contributed to River B (DB-1.0, DB-2.0 and DB-4.0) and one was in watershed C which contributed to River C (DC-1). Nine O&G discharge effluent stream sites were sampled downstream of the NPDES discharge point but upstream of the confluence point with the larger river (DA-4, DB-1.1, DB-2.1, DB-2.2, DB-3, DB-4.1). Two domestic groundwater wells were sampled for local groundwater impacts (Well 1 and Well 2). A Reference Tributary (Reference) was sampled to provide information on a true ephemeral stream unimpacted by O&G development and produced water discharges and remained dry for the majority of the study. Finally, an upstream background site (UDB-1.0) was sampled upstream of all known NPDES discharges on River B effluent stream. In subsequent figures within the text, distances are designated as negative and positive relative to the confluence point between O&G effluent streams and the larger receiving river (i.e. negative distance = upstream and positive distance = downstream of the confluence point). Specific locations remain undisclosed in coordination with access agreements with private landowners. McDevitt et al. (2018) previously described the study region with a focus on radium accumulation characterizations and mechanisms and McLaughlin et al. (2020b) described the DC-1 NPDES effluent stream with regards to organic pollutants and toxicity (McDevitt et al., 2018; McLaughlin et al., 2020a, 2020b).

In watershed A and C drainage areas, the NPDES facilities were the major water source for the ephemeral streams and thus no true background sample site existed. Areas located close to the perennial rivers were irrigated by utilizing dams and diversion channels to support grass hay fields, especially prevalent along River B. Much of the base stream flow in the produced water ephemeral streams is sourced from the NPDES-permitted O&G facilities and flows through well-drained tertiary and quaternary deposits comprised upwards of 20% calcium carbonate and 5% gypsum. Upstream River B and C soils contained even larger amounts of calcium carbonate upwards of 40% and gypsum upwards of 15% (NRCS, 2019).

O&G extraction in the region is well-established with development of some of the major formations dating back to the 1950s. Extraction wells studied were vertically drilled and hydraulically fractured for increased permeability and enhanced oil recovery (EOR). Five formations are the major reservoirs of O&G within the study area, but O&G reservoirs are present in nearly every formation. The five major reservoirs, from youngest to oldest are Mesaverde, Nugget, Chugwater, Phosphoria, and Tensleep. Due to the age of the geologic formations and history of O&G in the region, most of the many O&G formations produce large volumes of wastewater per barrel of oil equivalent, creating an excess of water that must be treated prior to discharge. In the US, average O&G wells produce

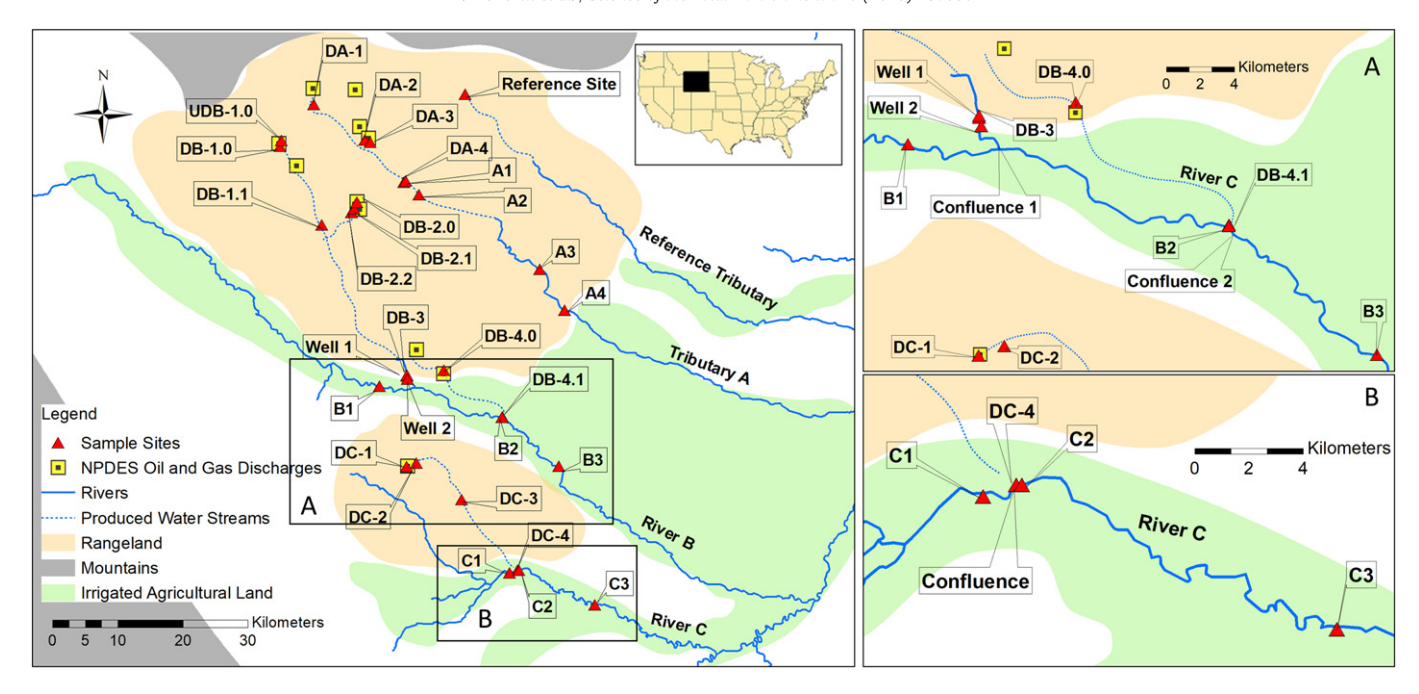


Fig. 1. Map of the study region located in Wyoming, USA. 30 GPS-located sites including 7 NPDES facilities within 3 0&G fields were sampled during 10 sampling events from 2013 to 2016. The NPDES discharges were located in dry upstream drainage regions and emptied into 3 larger rivers, A, B, and C. Tributary A is a smaller tributary channeling mainly produced water while River B and C represent large perennial rivers in the region with headwaters in upstream mountain regions. Approximate mountain ranges, cattle rangeland/sagebrush and irrigated agricultural land were drawn from aerial satellite images. A) and B) illustrate the confluence points of River B and River C with their respective produced water stream drainages.

7–10 barrels (1111–1588 L) of produced water to every barrel of oil generated (Guerra et al., 2011). In this region of Wyoming, from reported permit ratios, some wells are producing over 100 barrels (15,900 L) of produced water for every barrel of oil. Beneficial use exemptions of these produced waters allow companies to continue to operate because production would likely be economically unviable if added treatment was required prior to discharge to the environment. The 6 actively operating O&G NPDES discharges in this study alone cumulatively discharge approximately 7.9 million gal per day (29.8 million L per day) of produced water or 2.9 billion gal per year (10.9 billion L per year) (McDevitt et al., 2018).

According to their permits, NPDES facilities treated produced water using basic oil-gas-water separation technologies (pressure chamber, three phase separator, and heater treater) and a series of settling and skim tanks/ponds where excess oil could be removed prior to discharge to frequently dry ephemeral stream beds. Inorganic discharge regulations for the NPDES facilities are limited to specific conductance of 7500  $\mu$ S/cm, TDS of 5000 mg/L, chloride of 2000 mg/L, sulfate ranging between 2500 and 3000 mg/L depending on the permit accessed, radium-226 of 60 pCi/L, and a pH range between 6.5 and 9.

Stream gauge discharge data for all three river systems for the years 2013 to 2016 was accessed through the publicly available USGS National Water Information System (https://waterdata.usgs.gov/nwis/rt). USGS stream gauge stations located in the larger Tributary A, River B and River C indicated consistent flows across sampling events apart from June 2016 which represented an outlier peak flow on River B and River C likely due to heavy snowmelt from mountainous headwaters. Stream gauge discharge statistics are included in Figs. S1 and S2.

Specific conductance, pH, temperature, and dissolved oxygen were measured in the field at each location using a Hydrolab field meter. Water samples were collected and field filtered with 0.45  $\mu m$  cellulose acetate membrane filters and stored for cation and trace metal analysis using nitric acid to a pH <2. All samples were also stored in sealed, plastic bags in coolers with ice after collection and in a refrigerator at 4  $^{\circ} C$  in the laboratory. Field duplicates were collected for data quality assurance.

# 2.2. Surface water analysis

Major cations were measured by Inductively Coupled Plasma Optical Emission Spectrometry (ICP-OES) and trace metals by Inductively Coupled Plasma Mass Spectrometry (ICP-MS). Major anions (bromide, chloride, fluoride, and sulfate as  $SO_4^{2-}$ ) were measured by Ion Chromatography. Bicarbonate was measured by titration. Samples from May and October 2013 were not measured for alkalinity in the laboratory. For this subset of samples alkalinity was estimated by calculating the concentration from the cation-favored charge balance difference.

Oxygen and hydrogen stable isotopes of August and October 2016 water samples were measured on a LGR model DLT-100 laser water isotope analyzer located at University of North Carolina at Charlotte and reported as per mil ratios (‰) relative to Vienna Standard Mean Ocean Water (VSMOW). The results were then plotted relative to the global meteoric water line and local meteoric water line reported for Wyoming (Craig, 1961; Kendall and Coplen, 2001).

Prior to isotope measurement, strontium and lithium concentrations in a subset of surface water samples were measured on the Thermo Xseries II Inductively Coupled Plasma Mass Spectrometer (ICP-MS) located at the Penn State University Energy and Environmental Sustainability Laboratories (EESL) to achieve lower detection limits.

Radiogenic strontium isotopes ( $^{87}\text{Sr}/^{86}\text{Sr}$ ) were determined at Penn State by processing 250 ng of strontium in October 2016 water samples (n = 24). Samples were dried in Teflon vials at approximately 70 °C until no moisture remained before re-dissolving the sample in 1 mL of 2 N double distilled trace nitric acid. Samples were then purified concurrently with 250 ng Sr from IAPSO seawater standard and NIST SRM 987 using a prepFAST and Eichrom strontium-specific resin columns. Yield check aliquots were drawn from prepFAST permeate to process 10 µg/L in 8 mL of 18.2 M $\Omega$ ·cm water and measured on the Thermo Xseries II ICP-MS. Yield checks confirmed >98% mass recovery through the column.  $^{87}\text{Sr}/^{86}\text{Sr}$  ratios in samples and standards were measured on the ThermoFisher Scientific Triton Plus thermal ionization mass spectrometer (TIMS) also located at Penn State University EESL. During measurement SRM 987  $^{87}\text{Sr}/^{86}\text{Sr}$  was 0.710261  $\pm$  8E-6 (2SD) compared to an expected 0.710254 and IAPSO  $^{87}\text{Sr}/^{86}\text{Sr}$  was 0.709177  $\pm$  6E-5

(2SD) within the expected range of 0.709134-0.7093. Long-term laboratory average  $^{87}$ Sr/ $^{86}$ Sr of SRM 987 is 0.7102622  $\pm$  9E-6 and long-term average  $^{87}$ Sr/ $^{86}$ Sr of IAPSO is 0.7091928  $\pm$  9E-6.

Lithium isotopes (<sup>7</sup>Li/<sup>6</sup>Li) were also measured at Penn State on October 2016 water samples (n = 24) by chemical separation of lithium using cationic resin (2 mL resin bed of AG50W-X12, 200-400 mesh in a 9 cm high Bio-Rad column with a hydrophilic frit) and 0.2 N HCl. 150 ng of lithium was processed in each sample. Sample volumes were then dried on a hotplate in Teflon vials at approximately 70 °C before re-dissolving in 0.2 mL of double distilled 0.2 N HCl for column loading. Yield check aliquots were drawn from permeate and measured on the Thermo Xseries II ICP-MS and indicated >96% mass recovery through the column. Duplicate samples were processed and while one sample yielded 96% recovery, the other yielded 100% and their  $\delta^7 \text{Li}$ were 9.99% and 9.55% within  $\pm 0.5\%$  (2SD). Because of this we included the 96% yield sample. Only four of the 24 samples yielded <98% recovery. Yield percentages were included in Table S1. <sup>7</sup>Li/<sup>6</sup>Li ratios in samples and standards (Alfa Asar and SRM 3129a) were run simultaneously on the Neptune multi-collector ICP-MS located at Penn State University EESL, Samples were bracketed by 2 blanks and 2 IRMM-16 standards (NIST replacement for LSVEC) for a blank correction and to calculate the  $\delta^7$ Li as a per mil deviation from the IRMM-16 standard. IAPSO seawater method standard produced an isotopic composition of  $30.62 \pm 0.33\%$  (2SD). Average SRM 3129a  $\delta^7$ Li was 6.41  $\pm$  0.36% (2SD) (n = 15) and average Alfa Asar was  $80.85 \pm 0.24\%$  (2SD) (n = 14). The analytical precision for  $\delta^7$ Li was <0.5% (2SD).

Sulfur isotopes of sulfate  $(^{34}S/^{32}S_{SO4})$  were measured on the October 2016 sampling event surface water samples (n = 18) at the Stable Isotope Laboratory, University of Tennessee. Samples were filtered and acidified to pH 3 using HCl to remove bicarbonate/carbonate ions and avoid precipitation of witherite (BaCO<sub>3</sub>). 10 mL of 10% barium chloride solution was then added to precipitate dissolved sulfate via barite (BaSO<sub>4</sub>) precipitation (for most samples this was achieved by precipitating 10-50 mL of sample, though background river samples required at least 1 L of sample) to obtain at least 0.5 mg of BaSO<sub>4</sub> for isotope analysis. Precipitate was rinsed several times in order to remove chloride and other ions and then dried between 80 and 100 °C. The precipitate was then packed into a tin capsule with 1-5 mg of vanadium pentoxide  $(V_2O_5)$  to allow for a complete combustion of the sample inside the Costech elemental analyzer (EA) coupled to a Delta Plus XL IRMS. The analytical precision for  $\delta^{34}$ S was <0.3% and the standard used to normalize ratios was V-CDT (Canon Diablo Triolite).

Delta values for both lithium and sulfur isotopes of sulfate were calculated as per mil deviation from the respective standard using the following formula:

$$\delta(\%) = \left(\frac{\textit{Ratio}_{\textit{sample}}}{\textit{Ratio}_{\textit{standard}}} - 1\right) * 1000 \tag{1}$$

# 2.3. Data analysis and statistics

Field duplicate samples were collected and analyzed for 19 samples. Major anions and cations were within 2% RSD for all samples with a few exceptions for F, K, and Ba at concentrations near the detection limit. Samples with major anion/cation charge balances >15% difference were not included in the statistical analysis. There were four samples out of 247 total samples (<2% of samples) that did not meet this criterion, two of which were located at the Reference sample site due to a lack of available water sample for anion IC analysis as well as DB-4.1 in July 2014 and DA-3 in October 2015. 60 samples had charge balances >5% - 16 samples within 6% difference, 39 samples between 6 and 10% difference and 5 samples between 10 and 13% difference. Of those, 32 samples were collected on River B and C with low TDS and higher alkalinity compositions, making measurement challenging (Fritz, 1994).

USGS Produced Water Database data for all regional O&G formations was filtered similarly to surface water samples, keeping only data points within 15% charge balance difference. For simplicity, dominant cation and anion compositions were analyzed and used to determine formation water types. This process was also used to analyze the water types of the streams studied. Anions/cations comprising 50% or more of the total anion/cation milliequivalents were classified as dominant, and if a second anion/cation was >30% of the total anion/cation milliequivalents it was also listed in the water type characterization. Standard water type characterization (Back, 1960) was also completed and included in Table S1. Regression analysis, ANOVA, Pairwise Wilcoxon rank sum, and Kruskal-Wallis rank sum statistical tests for significance were determined using R statistical software (Version 0.99.486).

#### 3. Results and discussion

### 3.1. Characterization of NPDES effluent discharges

From water sample data (Table S1), Tributary A NPDES discharges (DA-1, DA-2 and DA-3) are characterized by Ca-Na-HCO<sub>3</sub>-SO<sub>4</sub>-Cl and Ca-Na-SO<sub>4</sub>-Cl-HCO<sub>3</sub> water types. River B and River C NPDES discharges (DB-2.0, DB-4.0 and DC-1) are dominated by water types enriched in sodium and sulfate. NPDES discharge DB-1.0 was the only NPDES discharge to be enriched more in chloride than sulfate and had the highest TDS measured in the study upwards of 10,000 mg/L, though this facility ceased discharging O&G effluents in the latter half of the study. Water type is an important O&G effluent characterization difference compared to the regional River B and C water types distinctly enriched in Ca-Na-HCO<sub>3</sub> type waters likely derived from calcium carbonate and gypsum-rich riverine sediments and drainage area soils (NRCS, 2019). The majority of the sampled effluent water types do not represent the more common sodium-chloride water types that dominate western, and eastern, produced waters (Guerra et al., 2011). From NPDES permits, multiple formations were drilled within the same O&G field and processed at a given NPDES facility. NPDES facilities DA-1, DA-2 and DA-3 processed produced waters derived from the Madison, Tensleep, Phosphoria, Embar, Dinwoody and Amsden formations. NPDES facilities contributing to River B and C derived produced waters mainly from the Nugget, Tensleep and Phosphoria formations. Compiled, charge balanced, USGS Produced Water Database data for the regional O&G formation water chemistry, pre-treatment, is included in Table S2. A stratigraphic column of regional formations is included in the Supplemental Information.

In general, NPDES effluents from DA-1, DA-2, DA-3 and DC-1 (though most were on average above 1000 mg/L) exhibit lower TDS concentrations than their published USGS pre-treatment produced waters, potentially due to surface water dilution during formation flushing processes in EOR and scaling within the oil-gas-water separation process. However, NPDES discharges DB-1.0, DB-2.0 and DB-4.0 exhibit TDS concentrations (all approximately >4000 mg/L) similar to USGS published formation data even after treatment. Produced water treatment in the study region is not intended for inorganic treatment prior to discharge. The high TDS concentrations in NPDES effluents may cause issues for downstream water quality and intended beneficial uses with natural mechanisms potentially enhancing TDS concentrations further.

### 3.2. Salinity increases with time and distance

TDS was plotted versus time (2013–2016) for the most downstream sample site on each of the larger streams (A4, B3 and C3) (Fig. 2A) and the most upstream sample site (A1, B1 and C1) (Fig. 2B) including the TDS data collected during the outlier peak June 2016 discharge. Though the outlier peak flow in June 2016 represents natural discharge variation, plots and statistics excluding the peak June 2016 flow are included

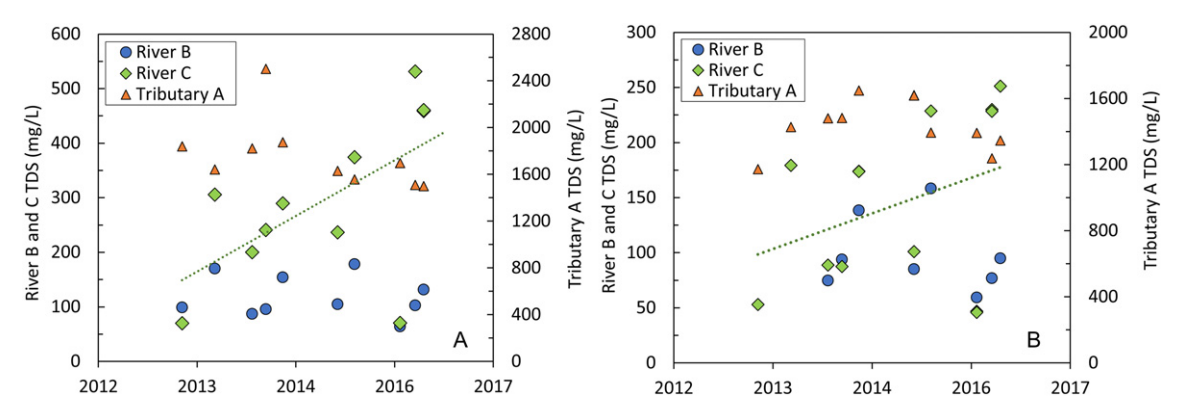


Fig. 2. TDS concentrations plotted versus time including June 2016 peak flow data for (A) downstream river sample points (A4, B3, C3) and (B) upstream river sample points (A1, B1, C1). While TDS concentrations increased in both River B and C, only River C downstream at C3 experienced a significant increase in TDS from 2013 to 2016. Note that the upstream Tributary A sample is not a true upstream site with respect to the O&G produced water stream confluence.

in Fig. S3 for a representative comparison of synoptic sampling conditions. All major and trace element data is included in Table S1. Tributary A TDS concentrations did not significantly change with time (p > 0.05) though its concentrations remained a magnitude higher than in River B and C, upwards of 2500 mg/L – 5 times the drinking water TDS secondary standard and approaching the upper limit of what is considered safe for agriculture. River C, however, had a TDS concentration of 70 mg/L during the first sampling event in 2013, then values were between 200 and 375 mg/L in 2013–2015. A TDS value of 70 mg/L was also recorded in June 2016 during a peak flow, followed by the two highest TDS values recorded in the study in August and November 2016 upwards of 532 mg/L.

Though Tributary A did not have significant TDS increases with time, there were significant increases in TDS with increasing distance downstream (A1 to A4) from an average 1438 mg/L at A1 to an average 1757 mg/L at A4 (p < 0.01 and  $R^2 = 0.41$ ). Chloride, sulfate, sodium, calcium, and hardness increased significantly with increasing distance downstream on Tributary A (p < 0.05). Though average concentrations of major anions and cations consistently increased on River B from upstream site B1 to downstream site B3 (average TDS increased from 98 to 199 mg/L) for all sampling events, no increases were determined statistically significant with distance. In addition to increasing TDS with time, River C TDS also increased with distance downstream of the O&G effluent stream confluence from upstream C1 average 145 mg/L to 295 mg/L downstream at C3 (p < 0.01,  $R^2 = 0.28$ ). River C sodium, sulfate, fluoride, magnesium, strontium, and manganese concentrations statistically increased with increasing distance from C1 to C3 (p < 0.05). However, no significant differences were determined for calcium or chloride. Another study located in Wyoming described increasing TDS concentrations in rivers driven by calcium, magnesium, and sulfate, likely sourced from dissolution of native soils caused by increased soil erosion from watershed-scale O&G development (Bern et al., 2015). Tributary A TDS concentrations upwards of 2500 mg/L are unacceptable for use a drinking water source. Wells 1 and 2 indicate salinity impacts from the losing nature of the bordering NPDES effluent stream with TDS averages between 800 and 1200 mg/L, almost two times the secondary TDS standard. Significant TDS increases with distance pose serious questions for reservoir water quality as a municipal drinking water source that is located downstream.

The high TDS concentrations mainly comprised calcium, sodium, and sulfate as presented by the strong linear relationships in Fig. 3. Strontium correlated strongly with calcium concentrations (Fig. 4A), boron with chloride (Fig. 4B), and lithium with sodium when grouped by watershed. Sodium and sulfate pose issues for agricultural O&G beneficial use. Irrigation with elevated sodium can cause increasing Sodium Absorption Ratios (SAR), which can inhibit crop yields and irrigation efficiency (Bern et al., 2013). Livestock drinking water elevated in sulfate and sulfides can cause diarrhea and even mortality at concentrations

above 2000 mg/L (Cammack et al., 2010; Gould et al., 1991; Kandylis, 1984). Currently, sodium concentrations are not monitored within NPDES regulatory limits and sulfate concentrations regulated between 2500 and 3000 mg/L are above what is considered chronically safe for livestock that frequently range in close proximity to the NPDES outfalls. Additionally, sulfate concentrations increase along the NPDES effluent stream with three-fold increases from NPDES site DC-1 to effluent stream site DC-4 approximately 32 km downstream and with 1.5-fold increases between NPDES site DB-2.0 to DB-2.2 only 2 km downstream. NPDES regulatory limits to date do not take into consideration potential evaporative effects along effluent streams post-discharge in a semi-arid environment.

Linear regressions were performed of measured TDS concentrations for each stream's most downstream sample point (all of which best correlated to the stream gauge location) against the USGS stream gauge flow data for sampling events. For all three stream systems no significant relationship was established between stream flow and TDS both including and excluding the outlier June 2016 discharge data (p > 0.05). Though more robust analyses can be completed on the concentration-discharge relationships, as evidenced in other regional studies, there are no USGS stream gauges recording any chemical parameters in the study region (Clark, 2012; Clark and Davidson, 2009). The absence of continuous specific conductance measurements is a major challenge in this region and leads to our limited synoptic sampling dataset of 10 sample dates over 4 years, making cause and effect analysis difficult utilizing more traditional geochemical techniques (Bern et al., 2015).

Many major U.S. watersheds experience pH increases simultaneously with salinization (Kaushal et al., 2018b). In this study, pH did not change significantly with time at downstream river sites (A4, B3 and C3) and instead fluctuated within a narrow range for all three study streams as seen in Fig. S4. Tributary A (all sites A1-A4) experienced a significant decrease in alkalinity with time (not distance) from 2013 to 2016, (p < 0.05,  $R^2 = 0.11$ ), opposite nationwide salinization trends with increasing alkalinization (Fig. S5). River B (all sites B1-B3) experienced no significant changes in hardness (as CaCO<sub>3</sub>) nor alkalinity from 2013 to 2016. However, River C (all sites C1-C3) which exhibited the largest TDS increase with time in this study, increased significantly in both alkalinity (p < 0.05,  $R^2 = 0.11$ ) and hardness (p < 0.05,  $R^2 = 0.17$ ) with time, similar to published salinization syndrome trends (Kaushal et al., 2018b). Additionally, alkalinity and hardness significantly increased with distance in River C. Average alkalinity concentrations increased from 84 mg/L at C1 to 122 mg/L at C3 (p < 0.05,  $R^2 = 0.14$ ) and average hardness concentrations increased from 113 mg/L at C1 to 196 mg/L at C3 (p < 0.01,  $R^2 = 0.23$ ). This observation also agrees with another Wyoming study that found coal-bed methane impacted watersheds such as the Powder River had increasing alkalinity due to the added discharges of sodium and bicarbonate to streams (Clark, 2012).

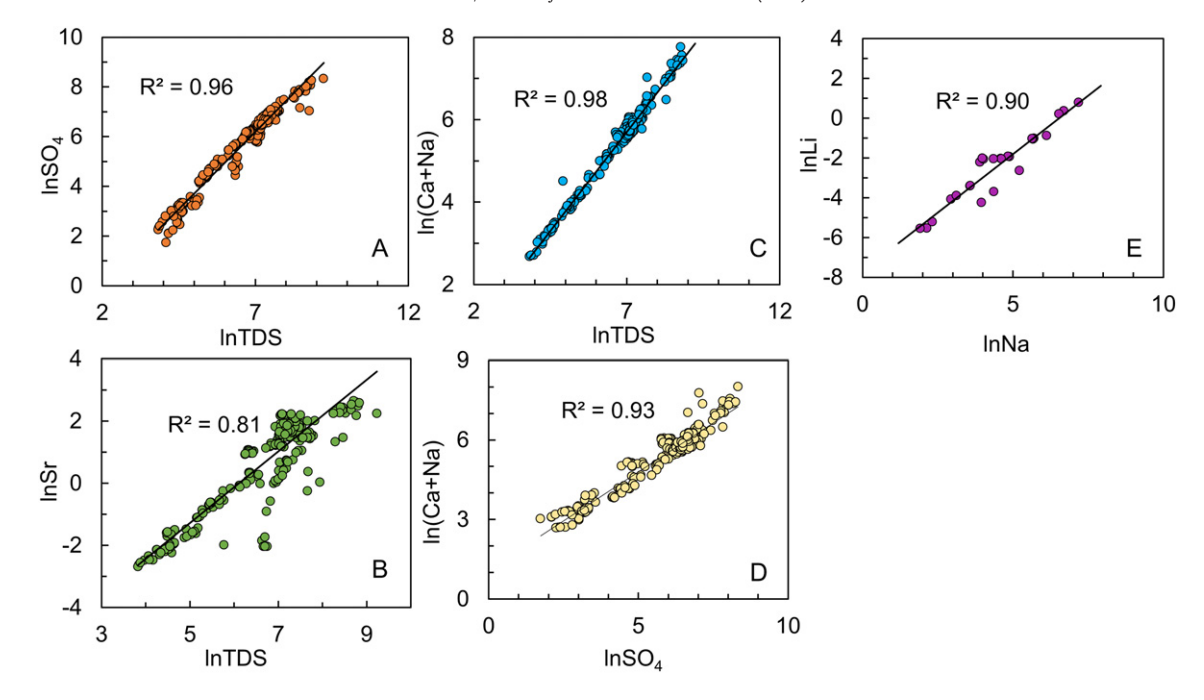


**Fig. 3.** Natural log of (A) SO<sub>4</sub>, (B) Sr, and (C) Ca + Na concentrations plotted versus the natural log of TDS and (D) natural log of Ca + Na concentrations versus natural log of SO<sub>4</sub> concentrations indicate the major individual contributing ions to TDS are SO<sub>4</sub>, Ca and Na with strong linear correlations. Sr, in general, is not a major component of the high TDS measured. (E) Li tracks closely with Na indicating Li potentially provides a good source tracker of Na sources.

# 3.3. Br/Cl and B/Cl molar ratios and $\delta^{18}$ O indicate evaporation

Many salinization studies have utilized the conservative environmental behavior of Br, B and Cl to elucidate salinity sources, especially for chloride driven salinization (Bouchaou et al., 2008; Lgourna et al., 2014; Vengosh, 2013; Warner et al., 2013b). O&G NPDES effluents (DA-1, DA-2, DA-3, DC-1 and DB-2.0) had Br/Cl molar ratios ranging from 0.0003 to 0.014, much wider ranging than those reported from Appalachian O&G brine ranging from 0.0024 to 0.0076 (Warner et al., 2012). It should be noted that reliable Br measurements above detection were only included for samples collected in August and November 2016 and may not fully represent all sampling conditions. Downstream river (C2, C3 and B2, B3) and upstream drainage (UDB-1.0) sample sites reflected higher Br/Cl molar ratios than NPDES discharges and effluent streams, upwards of 0.056 and 0.084, respectively. Groundwater wells reflected Br/Cl molar ratios on average 0.011, aligning with the effluent stream at site DB-1.1 with a Br/Cl molar ratio of 0.016 and indicating mixing and/or contribution from the nearby O&G effluent stream. Fig. S6 illustrates the inverse relationship between Br/Cl molar ratios and, interchangeably, TDS or Cl concentrations on River B and C while Tributary A samples plot similarly to the low Cl, high TDS O&G effluents with low Br/Cl molar ratios. The clear distinctions between River B and C Br/Cl and O&G effluents allows for calculation of end member mixing curves (Fig. 5) from which <1% of O&G effluent mixing is impacting the Br/Cl molar ratios of River B and <5% in River C. As TDS increased with distance along Tributary A, Br/Cl molar ratios remained consistently low, likely indicating evaporation of O&G effluent as the source of Tributary A salinization 60 km downstream of NPDES discharges (Fig. 6). Tributary A TDS increased with distance downstream consistently each sampling campaign (Fig. S7). River B and C do not exhibit trends as clear as in Tributary A, likely due to mixing with the estimated small water contributions from high TDS O&G effluent streams (Fig. S8). Log transformed Br/Cl molar ratios were plotted versus distance for comparison (Fig. S9) and reflect similar trends with less variability in Br/Cl molar ratios plotted along River B and C. Log transformed Br/Na and Br/SO<sub>4</sub> molar ratios were also plotted versus distance to reflect

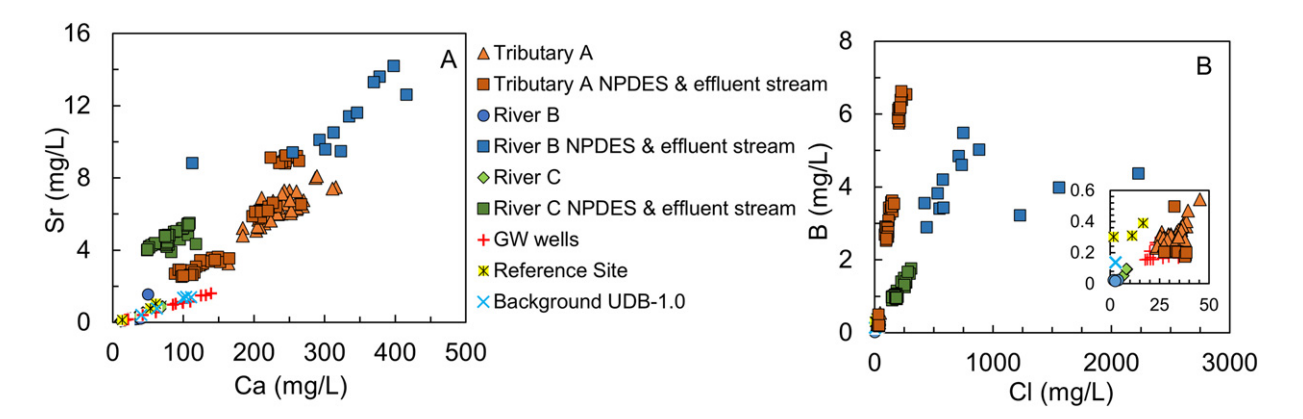


Fig. 4. (A) Strontium versus calcium and (B) boron vs chloride concentrations correlate linearly when categorized by larger Tributary A, River B and River C and their subsequent NPDES discharges and effluent streams. Reference site, background UDB-1.0, groundwater (GW) wells, and River B and C have low concentrations of all constituents while NPDES discharges and O&G effluent streams have relatively higher concentrations of all ions. Note that Tributary A sites plot similarly to the Tributary A NPDES discharges and effluent stream. Boron concentrations are especially elevated in effluents draining into River B and C.

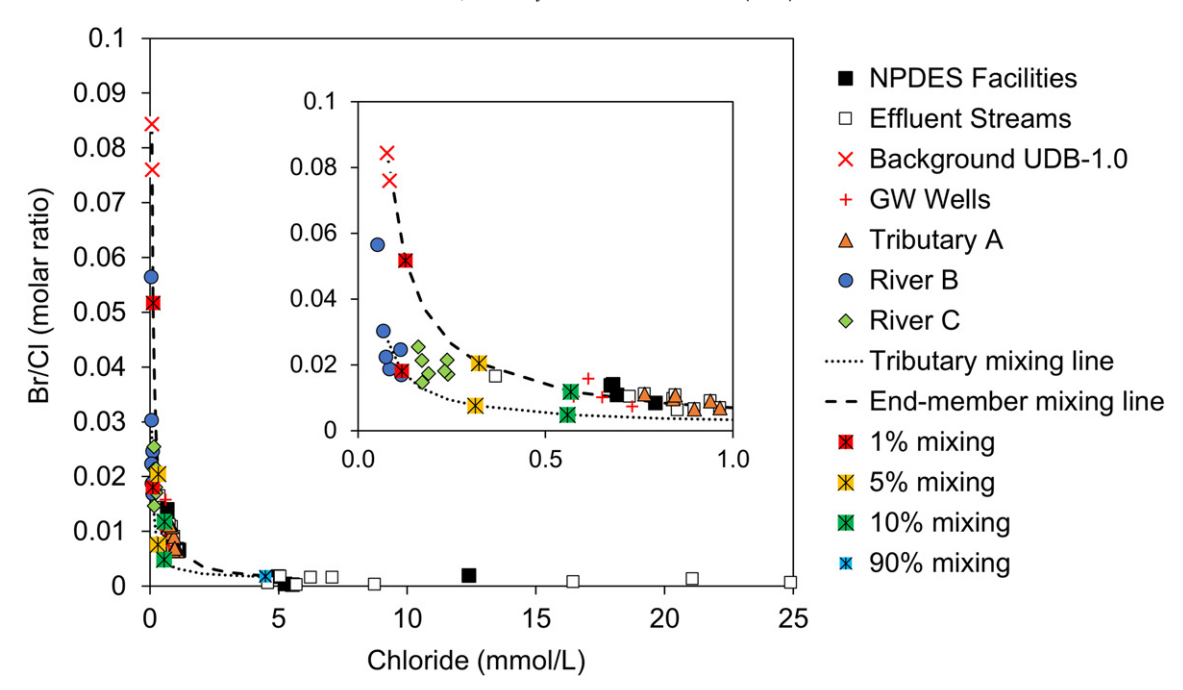


Fig. 5. Molar ratio Br/Cl versus chloride concentrations were plotted as individual watershed groupings. End member mixing curves were calculated from NPDES discharge DC-1 and upstream River B site B1 for the Tributary mixing line. DC-1 and background site UDB-1.0 were used to calculate the end member mixing line. Site UDB-1.0 had the highest Br/Cl ratio associated with low chloride concentrations. 1,5,10 and 90% mixing between 0&G effluent and end member water were also plotted. Mixing curves indicate that the Br/Cl ratios observed in the larger River B can be attributed to <1% O&G effluent mixing and between 1 and 5% in River C. GW wells indicate approximately 10% or greater mixing with O&G effluents. Note that Tributary A sites (A1-A4) plot similarly to NPDES facilities and effluent streams.

other major TDS components (Fig. S10). Both Na and SO<sub>4</sub> increase downstream, with higher increases in Na than SO<sub>4</sub> relative to Br. This could indicate ion exchange of Ca for Na or an additional salinity source downstream, notably in Tributary A and River C.

B/Cl molar ratios of all NPDES discharges ranged between 0.01 and 0.03 while all sites but background drainage sample site UDB-1.0 (0.13–0.16) fell in a similar range. Boron concentrations were elevated at NPDES discharges, especially those draining into River B (upwards of 5 mg/L), while Tributary A discharges and downstream river sites contained <1 mg/L B. Utilizing B/Cl and Br/Cl ratios a plot was recreated from Vengosh (2013) to try and fingerprint different sources of chloride concentrations (Fig. S11). Most samples fell within a bracket indicative of precipitation while River B and C O&G effluent fell within a bracket indicating hydrothermal waters, or simply waters having undergone water-rock interactions. Hydrothermal springs are present in this region of Wyoming and could be influencing the signatures of O&G formation water. Tributary A O&G discharges likely represent EOR processes and match the chloride signature of the local water being used to flush the O&G formations.

Additionally, the stable isotopes of oxygen ( $\delta^{18}$ O) and hydrogen  $(\delta^2 H)$  in water were plotted in relationship to the global meteoric water line (GMWL) ( $\delta^2 H = 8 (\delta^{18} O) + 10$ ) (Craig, 1961), and the local meteoric water line (LMWL) reported for Wyoming by Kendall and Coplen (2001) ( $\delta^2 H = 5.3 (\delta^{18} O) - 39.2$ ) (Fig. 7). The LMWL plots with a lower slope than the GMWL indicating regional evaporation due to the semi-arid climate. In general, the NPDES discharge samples exhibit more varied  $\delta^{18}\text{O}$  and  $\delta^{2}\text{H}$  than do the stream samples. For example,  $\delta^{18}$ O of O&G effluent samples within watershed B ranged from -18.21% to -13.49% (data from August to October 2016), while River B samples ranged from -16.38% to -15.70% (August 2016) data only). Similarly,  $\delta^{18}$ O of O&G effluents within watershed C ranged from -20.27% to -12.44% (August 2016 data only), whereas River C waters fell within the narrow range of -16.33% to -15.62% (August and October 2016 data). Overall, this implies that none of the O&G effluent streams in watersheds B or C is a volumetrically large water contribution to River B or C (but does not rule out significant solute

contributions), and also that Rivers B and C are not highly affected by downstream evaporation. In contrast,  $\delta^{18}$ O values of Tributary A stream waters are closer and more consistent to watershed A's O&G effluent inputs than were seen elsewhere in the study region (O&G effluent inputs -19.41% to -18.74%, Tributary A -19.19% to -17.06%). This suggests that other water inputs are not needed to produce the isotopic composition of Tributary A, although inputs of water derived from lower-elevation and/or summer precipitation, if they occurred, could also contribute isotopically enriched water to a stream. In addition, relatively constant Br/Cl molar ratios with distance on Tributary A provide no evidence of additional water inputs beyond O&G effluents. Rivers B and C align in their isotopic signature and plot closely with the LMWL, whereas Tributary A appears to plot slightly below or to the right of the LMWL, consistent with being more evaporated than regional river water. Moreover, the farthest downstream water sample in Tributary A exhibits the most enriched isotopic signature of watershed A in both August and October 2016, consistent with downstream evaporation in Tributary A. From Br/Cl molar ratios,  $\delta^{18}$ O and  $\delta^{2}$ H evaporation along Tributary A is causing O&G effluents, that meet NPDES regulations at the outfall, to not only exceed outfall regulations downstream where beneficial use of O&G effluent mainly occurs for irrigation and drinking water but also exceed aquatic life and livestock recommended limits. The larger perennial Rivers B and C dilute the effluent and aid in counteracting significant impacts to TDS from smaller volumetric contributions from O&G effluent streams. During periods of low river flow or periods of high NPDES effluent discharge, TDS impacts from O&G effluent streams could be exacerbated and require future monitoring.

# 3.4. Major elemental molar ratios, ${}^{87}Sr/{}^{86}Sr$ , and $\delta^{34}S_{SO4}$

lons of significance (Na, SO<sub>4</sub>, B, Sr and Ca) were normalized to conservative Cl for River C and River B (Figs. 8 & 9, respectively). While all major TDS constituents increased with distance between site C1 and C3 on River C, only SO<sub>4</sub> (51 to 136 mg/L), Na (10 to 25 mg/L) and Mg (9 to 18 mg/L) increased significantly (p < 0.05). These results remain consistent with Cl-normalized molar ratios. Na/Cl and SO<sub>4</sub>/Cl molar

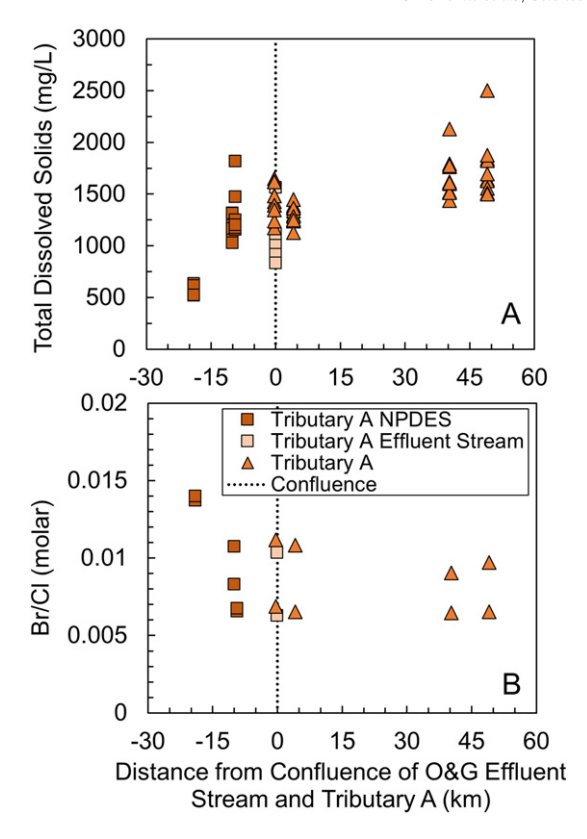


**Fig. 6.** Tributary A (A) TDS and (B) Br/Cl molar ratios plotted versus distance relative to the confluence between the O&G effluent stream and Tributary A. While TDS steadily increases with distance downstream of O&G discharges to the extent that downstream Tributary A sites have the highest TDS concentrations, upwards of 2500 mg/L, conservative Br/Cl molar ratios remain constant indicating evaporation of O&G effluents as the cause of increasing salinity along the Tributary. Differences in the Br/Cl molar ratio measured at each site are due to temporal differences in the August and October 2016 sampling events. Identical plots for River B and C are included in the Supplemental information

ratios increase from C1 to C3, opposite expected results if O&G effluent, with low Na/Cl and SO<sub>4</sub>/Cl molar ratios, caused elevated downstream River C TDS concentrations. B/Cl and Sr/Cl molar ratios also increase with distance downstream on River C, opposite of the expected influence from O&G effluent with lower ratios. River C O&G effluent stream

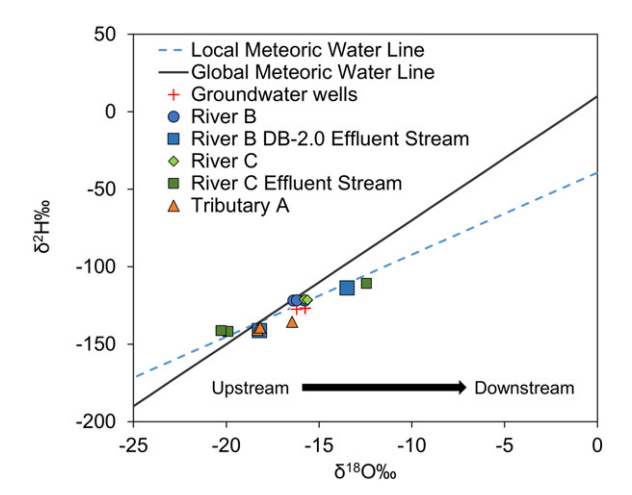


**Fig. 7.** Stable hydrogen and oxygen isotopes of water in each river or effluent stream are plotted relative to the global and local meteoric water lines determined for Wyoming. For all sites except two (River B DB-2.0 effluent stream), August 2016 data is shown. River B DB-2.0 effluent stream represents data collected in October 2016 due to not sampling the sites in August. Single-point effluent discharges are not plotted.

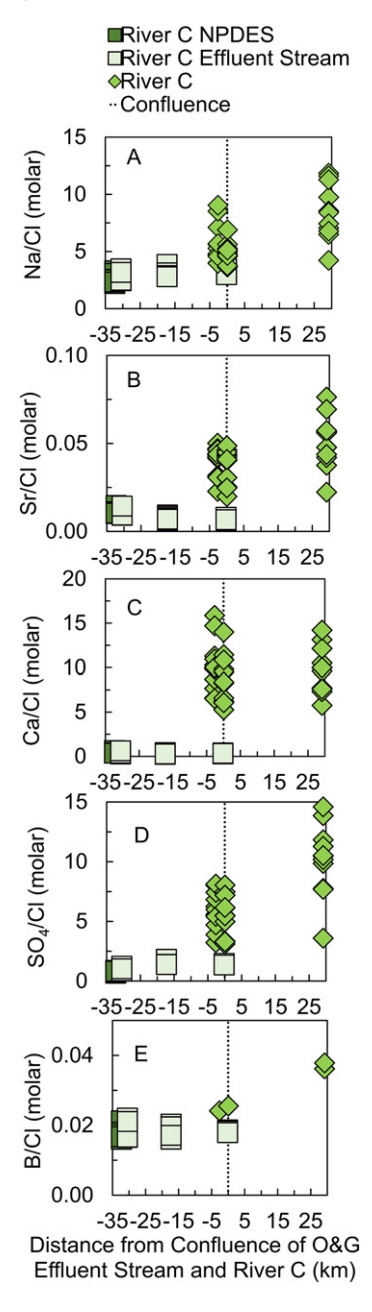


**Fig. 8.** Chloride normalized molar elemental ratios (A) Na/Cl (B) Sr/Cl (C) Ca/Cl (D) SO<sub>4</sub>/Cl and (E) B/Cl plotted versus distance from the confluence of River C and River C NDPES O&G discharges. Note that while there seem to be little impact on the River C site from upstream of the confluence to just below (C1 to C2), notably a slight decrease in the Sr/Cl and Ca/Cl ratios, downstream site C3 indicates an additional salinity source which is increasing the Na/Cl, SO4/Cl, Sr/Cl and B/Cl ratios not aligned with the lower O&G molar ratios

molar ratios (Na/Cl, Sr/Cl, Ca/Cl, SO<sub>4</sub>/Cl, B/Cl) remain relatively consistent with increasing distance from the NPDES discharge confirming further the importance of taking evaporative effects into account in NPDES discharge limitations. Ca/Na molar ratios decrease downstream on River C though Ca concentrations did not significantly increase with distance, indicating dissolution of gypsum is not the only source of increasing TDS and instead an additional Na source or ion exchange of Ca for Na (Fig. S12). Jin et al. (2010) reported increased calcite precipitation in a Wyoming stream impacted by increased calcium and sulfate concentrations derived from gypsum dissolution, a phenomenon that could explain decreased Ca/Na molar ratios. Though River B average concentrations of Na, SO<sub>4</sub>, Ca and Mg increase only slightly with distance downstream from B1 to B3, no increases were significant (p > 0.05).

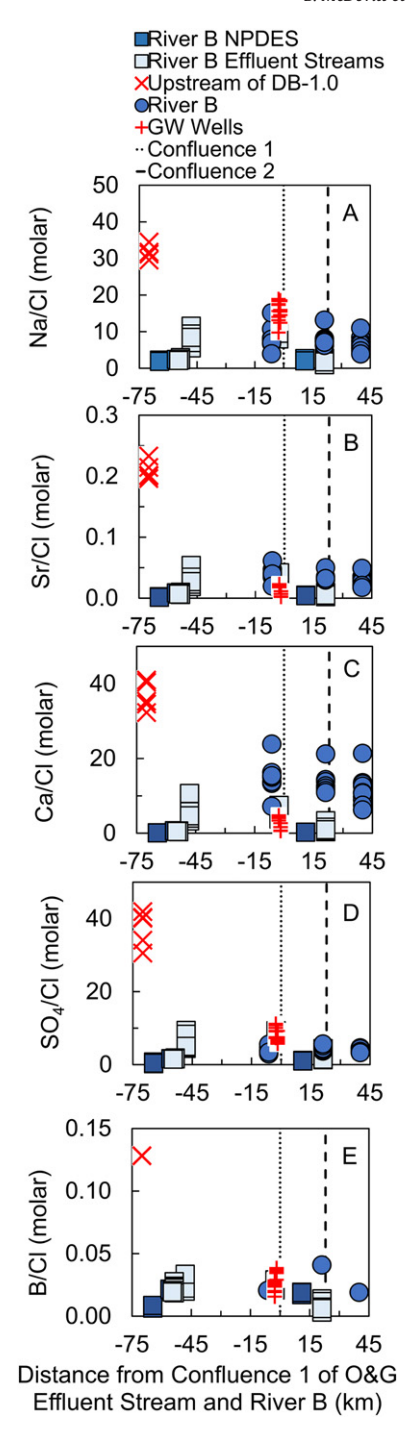


**Fig. 9.** Chloride normalized elemental molar ratios (A) Na/Cl (B) Sr/Cl (C) Ca/Cl (D) SO<sub>4</sub>/Cl and (E) B/Cl plotted versus distance from the confluence for River B. Note that ratios for the NPDES discharges are all lower than background and larger river ratios. Note that River B ratios remain relatively consistent from upstream to downstream of both confluences with O&G effluent streams.

Concurrently, Na/Cl, SO<sub>4</sub>/Cl, Sr/Cl and Ca/Cl remain consistent from upstream to downstream with seemingly little observable impact from O&G effluent TDS components leading to the need for <sup>87</sup>Sr/<sup>86</sup>Sr as a salinity tracer. Ca/Na molar ratios increase along both O&G effluent streams likely indicating soil gypsum dissolution, cation exchange of Na for Ca, or mixing with higher background UDB-1.0 waters.

 $^{87} \rm Sr/^{86} \rm Sr$  for River C NPDES discharge, DC-1, was 0.70964 and remained consistent along the length of the O&G effluent ephemeral stream, indicating evaporation of O&G effluent increasing TDS prior to the confluence with River C (Fig. 10). In other studies on O&G produced

water impacts <sup>87</sup>Sr/<sup>86</sup>Sr was used to distinguish specific formation sources. For example, the Marcellus Shale displayed lower ratios (0.710–0.711) than those observed in conventional produced waters in the same region and other sources of contamination such as acid mine drainage (0.7145–0.7146) (Chapman et al., 2012; Warner et al., 2013a). River C <sup>87</sup>Sr/<sup>86</sup>Sr upstream at C1 was 0.71092, which decreased to 0.71078 after the O&G confluence at C2, reflecting impacts from mixing with the low <sup>87</sup>Sr/<sup>86</sup>Sr signature from DC-1. Conservative mixing calculations estimate this mixing was low, with only 1% mixing of a DC-1 O&G signature with upstream C1 (Fig. 10C). However, farthest downstream C3 <sup>87</sup>Sr/<sup>86</sup>Sr likely reflects a salinity source other than O&G effluent as the ratio increases to 0.71223, more like the downstream River B ratio of 0.71225. Fertilizers have reported radiogenic <sup>87</sup>Sr/<sup>86</sup>Sr around 0.715 (Bentley, 2006) which could be sourced from agricultural return flows causing increasing  $^{87}\mathrm{Sr}/^{86}\mathrm{Sr}$  in the downstream River B and C. Dissolution of gypsum soils can likely be negated as a possible source of calcium because they exhibit less radiogenic ratios ranging from 0.70698 to 0.70778 (Denison et al., 1998). Background UDB-1.0 surface waters originating from the drainage regions, enriched in calcium carbonate minerals, reflected much lower <sup>87</sup>Sr/<sup>86</sup>Sr of 0.70844, similar to values reported in a creek in the Williston Basin and in the Juniata Creek in Pennsylvania, areas underlain by thick accumulations of limestone similar to the study area (Cozzarelli et al., 2016; Geeza et al., 2018). <sup>87</sup>Sr/<sup>86</sup>Sr ranging from 0.707 to 0.709 also reflect values reported for marine limestones and dolomites sourced from the Phanerozoic era (Bentley, 2006). River B O&G effluent reflected slightly higher 87Sr/86Sr to that of DC-1 with 0.71016-0.71050. Upstream River B, B1, 87Sr/86Sr was 0.71281 which decreased after the first confluence at B2 to 0.71228 and decreased again after the second confluence to 0.71225 at B3 (Fig. 11). While both O&G discharges and background waters reflect low 87Sr/86Sr compared to River B surface water, the O&G discharges have Sr and Ca concentrations of approximately 9 mg/L and 300 mg/L compared to average background of 1 mg/L and 84 mg/L, respectively. Conservative mixing calculations estimate <1% mixing with O&G effluents impacting downstream River B sites B2 and B3 (Fig. 11C). The <sup>87</sup>Sr/<sup>86</sup>Sr mixing calculations agree with those derived from the Br/Cl molar ratios. In the O&G discharges upstream of Tributary A <sup>87</sup>Sr/<sup>86</sup>Sr ranged from 0.70878 to 0.70957 (Fig. S13). Tributary A <sup>87</sup>Sr/<sup>86</sup>Sr varied little between 0.70868 and 0.70879 over a 60 km distance, indicating evaporation of O&G effluent increased Sr concentrations and not an ex-

Sulfur isotope composition of sulfate ( $\delta^{34}S_{SO4}$ ) in the surface waters may help further distinguish the non-O&G salinity source in the downstream River C. Dissolution of evaporites and rocks does not significantly alter the sulfur isotopic composition, and there is a vast difference between the  $\delta^{34}$ S of sulfates and sulfides. Therefore, sulfur isotopes can be used as a tracer of sulfate ions with respect to sulfate contributions from evaporite dissolution, oxidation of hydrogen sulfide and/or sulfide minerals, and mixing of waters with different sulfur isotopic compositions (Clark and Fritz, 1997; Porowski, 2014; Szynkiewicz et al., 2012). The O&G NPDES discharges upstream of River C and B had  $\delta^{34}S_{SO4}$  of +19.8 and +22.1% respectively, reflecting similar  $\delta^{34}S_{SO4}$  values reported in a petroleum study for similar formation waters (Figs. 10B & 11B) (Vredenburgh and Cheney, 1971). However, these discharges were sourced from Permian, Triassic and Upper Cretaceous formations and reflect higher  $\delta^{34}S_{SO4}$  compared to the  $\delta^{34} S_{SO4}$  of global Permian marine evaporites such as gypsum and anhydrite (+10.5 to +15%) (Claypool et al., 1980). The  $\delta^{34}S_{SO4}$  of Tributary A NPDES discharges ranged between +15 and +17% consistent with the range of  $\delta^{34} S_{SO4}$  reported for the Pennsylvanian and Mississippian formations in Wyoming (Vredenburgh and Cheney, 1971). All O&G effluent ephemeral streams indicate significantly lower  $\delta^{34} S_{SO4}$  prior to mixing at the river confluence. Because all NPDES discharges had high hydrogen sulfide concentrations the lower  $\delta^{34} S_{SO4}$  of O&G effluent in the stream is likely due to oxidation of hydrogen sulfide gas. The expected  $\delta^{34}S_{SO4}$  range from oxidation of hydrothermally-derived

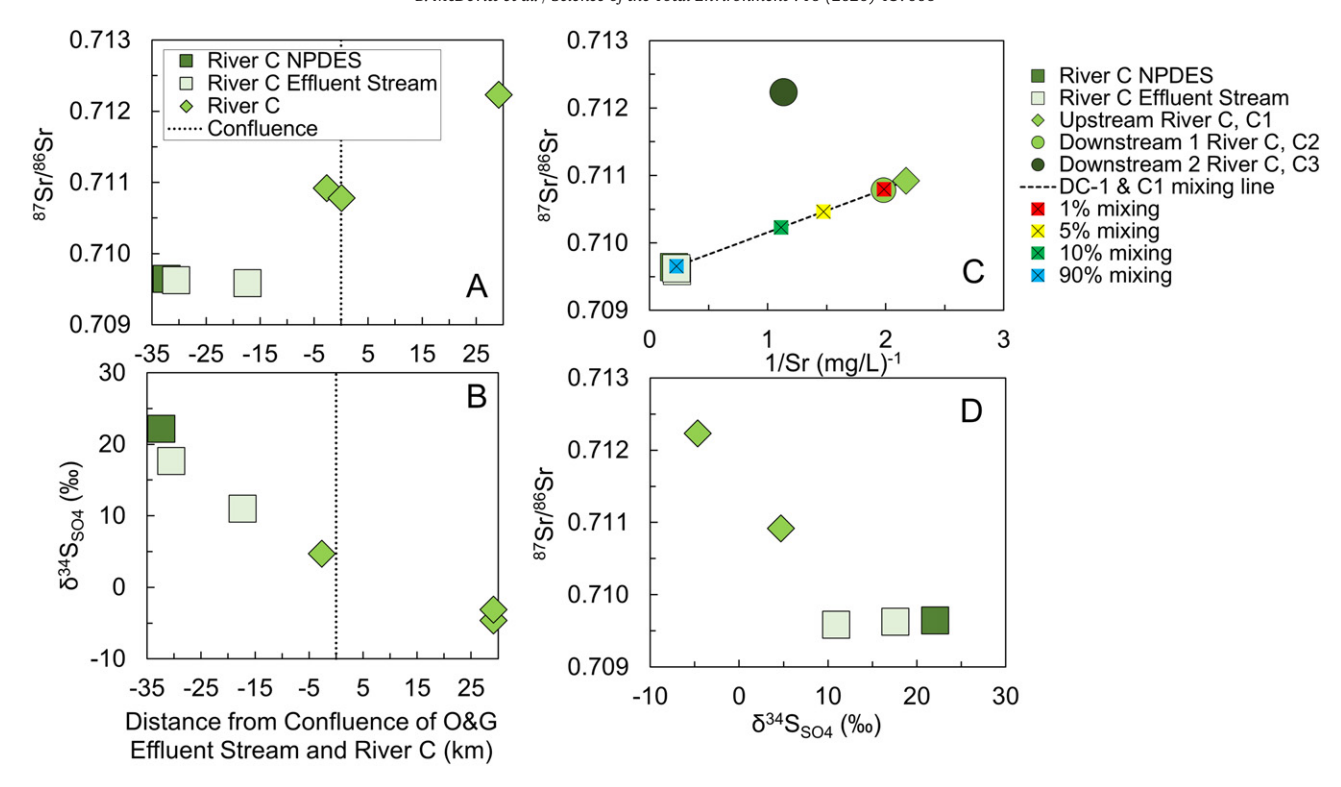


Fig. 10. (A)  $^{87}$ Sr/ $^{86}$ Sr and (B)  $^{34}$ S<sub>S04</sub> plotted versus distance from 0&G effluent stream confluence on River C and (C)  $^{87}$ Sr/ $^{86}$ Sr mixing curves versus 1/Sr.  $^{87}$ Sr/ $^{86}$ Sr indicate a slight decrease after the confluence from 0.71092 to 0.71078 but a large increase to a more radiogenic signature downstream to 0.71223, though 0&G effluent remains <0.710.  $^{34}$ S<sub>S04</sub> of the 0&G discharge decreases with distance indicating sulfide oxidation while  $^{87}$ Sr/ $^{86}$ Sr remain constant. From C1 to C3,  $^{34}$ S<sub>S04</sub> decreases from ~+5 to -5% which could indicate an additional sediment source different from upstream geology.  $^{87}$ Sr/ $^{86}$ Sr mixing curves indicate that there is 1% mixing with 0&G effluent on River C after the first confluence, but the C3 ratios do not fit the NPDES and upstream C1 mixing line trends also indicating an alternative strontium source. The  $^{87}$ Sr/ $^{86}$ Sr vs  $^{34}$ S<sub>S04</sub> plot (D) clearly shows steady  $^{87}$ Sr/ $^{86}$ Sr from the NPDES facility DC-1 on its effluent stream indicating evaporation while the decreasing, enriched,  $^{34}$ S<sub>S04</sub> indicates sulfide oxidation prior to mixing with upstream River C water with more depleted  $^{34}$ S<sub>S04</sub> in the range of global river waters at  $^{44}$ 7%.

hydrogen sulfide is -26 to -3% (Szynkiewicz et al., 2015). After mixing at the confluence, the Tributary A sulfate concentrations increase while  $\delta^{34}S_{SO4}$  remains relatively constant for nearly 60 km, reiterating evaporation (+8.7 to +8.2%) (Fig. S13B). The  $\delta^{34}S_{SO4}$  of River B decreases from upstream to downstream by 1%, though the  $\delta^{34}S_{SO4}$ stays in the range of meteoric waters and terrestrial evaporites (+3.7)to +4.7%). The  $\delta^{34}S_{SO4}$  of River C upstream remains +4.7% but downstream C3  $\delta^{34}$ S<sub>SO4</sub> decreases to approximately -4%, indicating potential contribution of sulfate from dissolution of shale-derived deposits enriched in biogenic sulfides with negative  $\delta^{34}S_{504}$  values (Lueth et al., 2005). A large percentage of stream sediments located downstream are derived from the local sandstones and shale, known to be enriched in sulfide minerals with lower  $\delta^{34}S_{SO4}$  (NRCS, 2019; Porowski, 2014). Terrestrial evaporites fall within a wide  $\delta^{34}S_{SO4}$  range of -15 to +10% so the decrease in  $\delta^{34}S_{SO4}$  and increase of TDS could also be a function of increased soil erosion or overland irrigation flow contributing to River C (Porowski, 2014).  $^{87}$ Sr/ $^{86}$ Sr and  $\delta^{34}$ SsO4, together, further demonstrate that the Tributary A salinity source is O&G effluents and that Rivers B and C are slightly impacted from O&G effluent (<1%). River C downstream TDS increases are likely due to enhanced soil erosion or agricultural return flows.

# 3.5. Li isotopes as a salinity tracer

Lithium provided a clearer distinction between NPDES discharges and the larger rivers with all discharges elevated at least an order of magnitude and up to three orders of magnitude in Li concentrations (i.e. 2.2 mg/L at DB-2.2 vs vs 0.014 mg/L at UDB-1.0 vs 0.004 mg/L at B1), tracking strongly with chloride concentrations. Lithium isotopes for NPDES discharges had a  $\delta^7$ Li tightly between 9 and 10% except for DA-2, which had a  $\delta^7$ Li of 12.3%. The only NPDES discharge that was

not analyzed for  $\delta^7$ Li was DB-4.0 because no water samples were collected there beyond 2014. However, its O&G effluent stream site DB-4.1 was analyzed and had the highest  $\delta^7$ Li measured of 22.0%, indicating a different O&G formation source than other NPDES discharges represented, a different treatment process, and/or enhanced waterrock interactions along the effluent stream (i.e. adsorption onto clay or coprecipitation with clay and other secondary minerals). Additionally, Li isotopes have a negative correlation to temperature with lower  $\delta^7$ Li associated with higher temperatures as could be the case for the  $\delta^7$ Li measured at most NPDES discharges (i.e. DC-1, DB-2.0) in the range of hydrothermal waters (Macpherson et al., 2014). The produced water treatment in a heater treater system could also alter the original produced water  $\delta^7 \text{Li}$ , causing a decreased  $\delta^7 \text{Li}$  in the NPDES effluent discharged to the effluent stream (Macpherson et al., 2014b). Fig. 12 depicts the  $\delta^7$ Li changes with distance. Tributary A exhibits an increase in δ<sup>7</sup>Li. <sup>6</sup>Li has been observed to fractionate by incorporation into calcite and aragonite minerals, in addition to adsorption or co-precipitation with clay and other secondary minerals, which subsequently remain significantly depleted compared to their enriched seawater growth solution (Marriott et al., 2004). Carbonate mineral precipitation is a dominating mechanism on the O&G effluent ephemeral streams with some grab sediments at NPDES discharges comprised of >97% calcium carbonate (McDevitt et al., 2018). Background UDB-1.0  $\delta^7$ Li was higher compared to NPDES discharges with a  $\delta^7$ Li of 14.8%. Rivers B and C did not demonstrate as clear of a  $\delta^7$ Li increase with distance downstream, indicating its limited application as a salinity tracer. Murphy et al. (2019) recently reported the limitations of  $\delta^7$ Li as a salinity tracer due to groundwater inputs to rivers but reported maximum Li concentrations were magnitudes less than observed in this study, in a watershed receiving more precipitation, and over 1000 km downstream. Oi et al. (2019) more similarly found that  $\delta^7$ Li was useful as a salinity source

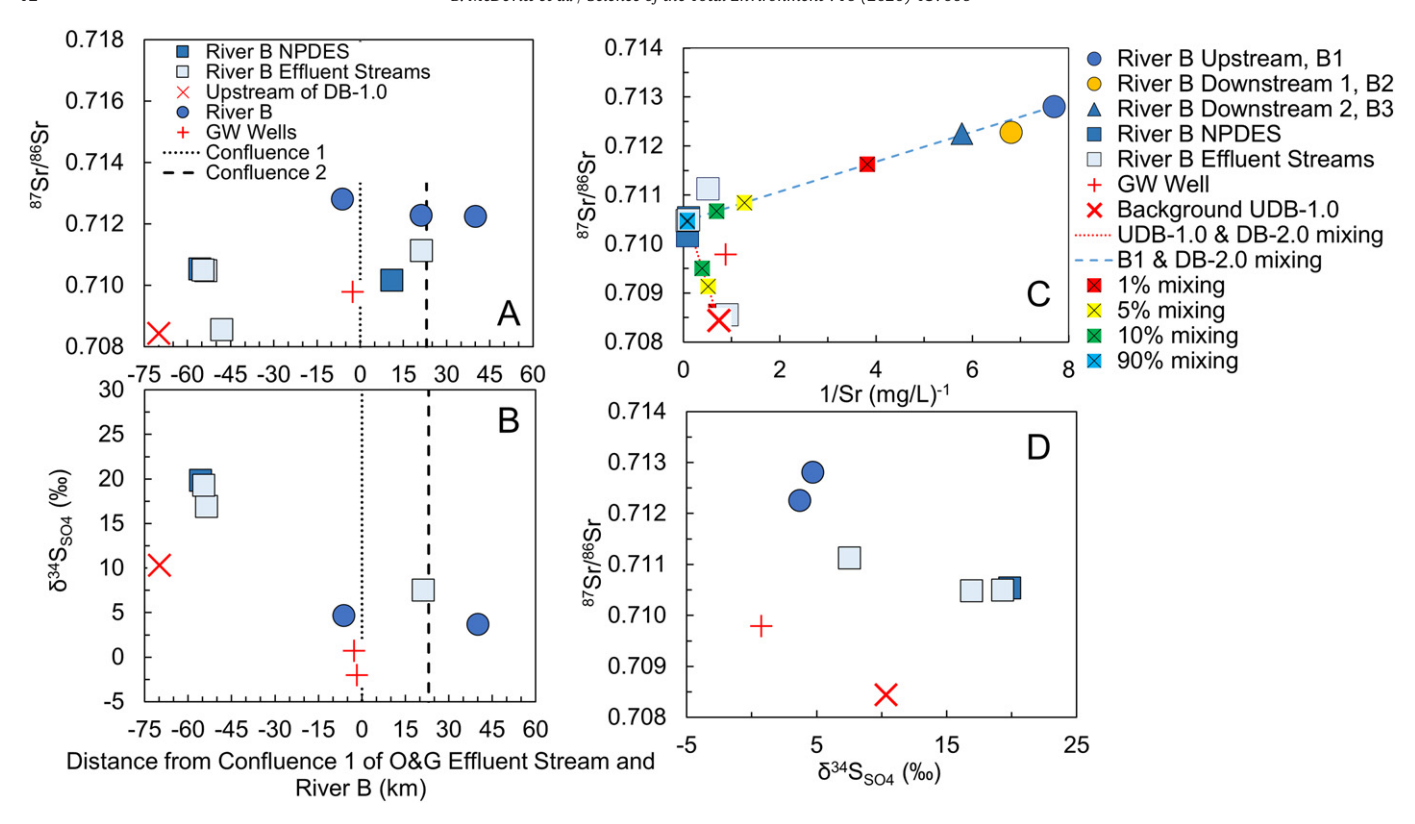


**Fig. 11.** (A)  $^{87}$ Sr/ $^{86}$ Sr and (B)  $^{84}$ S<sub>SO4</sub> plotted versus distance from confluence 1 on River B and (C)  $^{87}$ Sr/ $^{86}$ Sr mixing curves versus 1/Sr.  $^{87}$ Sr/ $^{86}$ Sr indicate a slight decrease after the first confluence from 0.7128 to 0.7123 and another slight decrease after the second confluence to 0.7122 due to impacts from 0&G discharges also with less radiogenic  $^{87}$ Sr/ $^{86}$ Sr signatures around 0.710 but with highest contributing Sr concentrations,  $^{84}$ S<sub>SO4</sub> allows for grouping of NPDES discharges from river and background waters but impacts are less clear due to the non-conservative nature of S and high fractionation factors associated with sulfide oxidation likely occurring on PW streams.  $^{87}$ Sr/ $^{86}$ Sr mixing curves indicate that there is <1% mixing with 0&G effluent on River B though there are impacts to the  $^{87}$ Sr/ $^{86}$ Sr ratio. The  $^{87}$ Sr/ $^{86}$ Sr vs  $^{34}$ S<sub>SO4</sub> plot (D) indicates steady  $^{87}$ Sr/ $^{86}$ Sr from the NPDES facility DB-2.0 on its 0&G effluent stream indicating evaporation while the decreasing, enriched,  $^{84}$ S<sub>SO4</sub> indicates sulfide oxidation prior to mixing with background UDB-1.0 and River B water with more depleted  $^{83}$ Sr/ $^{84}$ 

fingerprinting tool but fractionation ultimately limits salinity tracing capabilities.

### 4. Conclusions

Each of the three watersheds presented in this study represent different mechanisms and salinity sources responsible for their elevated TDS or increasing TDS concentrations with distance downstream and/or time. Because these watersheds ultimately contribute to a drinking water supply and O&G effluent is discharged as beneficial use for agriculture, further investigation proved necessary in order to best pinpoint salinity sources in the region. By using elemental ratios and a

variety of isotopic systems as salinity tracers the critical water management knowledge gap was narrowed and led to a better understanding of beneficial use of O&G produced water in a semi-arid environment where much of the beneficial use is practiced in the U.S. Tributary A is an O&G effluent stream along its entire length that experiences evaporation and concentrates O&G effluent that, at its source, would not be a major cause for concern to discharge, with regards to TDS. Downstream, Tributary A is not a suitable drinking water source due to high TDS concentrations upwards of 2500 mg/L, above the recommended limits as a water source for irrigation, and nearing limits recommended for livestock drinking water. Elemental ratios and strontium isotopes were sufficient for determining the source of salinity on Tributary A.

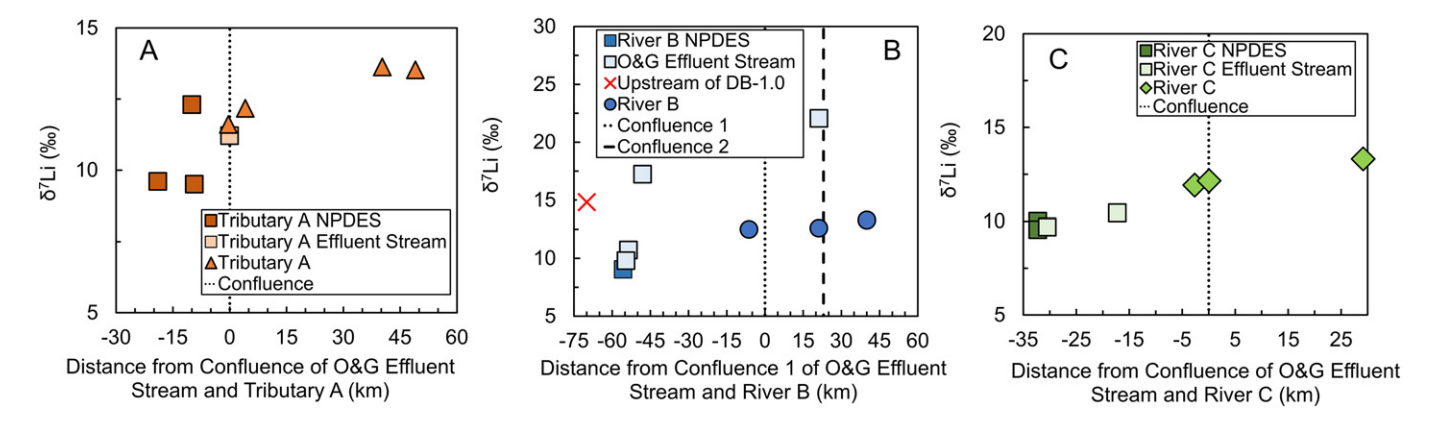


Fig. 12.  $\delta^7$ Li plotted versus distance for each of the watersheds, A, B and C. 0&G discharges consistently fall within 9–10% and exhibit increases along the 0&G effluent streams likely due to water-sediment interactions and carbonate mineral precipitation. River samples range consistently between 12 and 14% slightly depleted compared to the global river water  $\delta^7$ Li range.

River B which has increasing TDS (though not statistically significant) was impacted only slightly from O&G discharges. Elemental ratios and strontium isotopes were necessary for identifying impacts which indicated much <1% mixing of O&G effluent and River B to cause only slight changes to the  ${}^{87}\mathrm{Sr}/{}^{86}\mathrm{Sr}$ . In the future, if the volume of O&G effluent discharged increases, there is the potential to observe significant increases in TDS in River B from high TDS loads currently buffered by large dilution factors. Significantly increasing TDS in River C is most likely due to agricultural irrigation runoff or soil erosion downstream. Elemental ratios, strontium isotopes, and sulfur isotopes, combined, indicated slight O&G effluent impacts in River C but likely eliminated O&G as the source of worrisome TDS increases. Without strontium or sulfur isotopes O&G as a source of salinity downstream on River C may have been considered since elemental ratios were not adequate to confirm an alternative salinity source. Wherever multiple salinity sources and environmental mechanisms affect water quality, large tool kits are required in order to fingerprint sources and to understand how to best manage water supplies. The large tool kit becomes more imperative in semi-arid and arid areas where freshwater supplies are not ubiquitous. Salinization is a global phenomenon and issue for human and environmental health, energy production, agricultural yields, and the economics of drinking water supply. Utilizing an isotopic tool kit when elemental ratios prove inadequate prior to stakeholder disputes may be necessary to ensure the stability and longevity of global freshwater

Supplementary data to this article can be found online at https://doi.org/10.1016/j.scitotenv.2020.137006.

# **Declaration of competing interest**

The authors declare that they have no known competing financial interests or personal relationships that could have appeared to influence the work reported in this paper.

# Acknowledgements

The authors would like to acknowledge O&G operators and land-owners without whom sampling could not have taken place. We would thank Pennsylvania State University for the University Graduate Fellowship which provided student support as well as the Energy and Environmental Sustainability Laboratory (EESL) at Penn State for funding lithium stable isotopes analysis. NSF INTERN 1747807 and NSF CBET 1703412 funded the majority of this research. Additionally, this research was funded, in part, by the Environmental Defense Fund and Colorado State University Water Center. Additionally, we would like to thank Matthew Gonzales from the LIME lab at Pennsylvania State University for his help in measuring strontium and lithium isotopes; Anna Szynkiewicz from University of Tennessee for her laboratory's analysis of the sulfur isotopic compositions of sulfate concentrations; and Katherine Van Sice for her contribution of the stratigraphic formation column in the SI.

### References

- Ayers, R.S., Wescot, D.W., 1994. Water Quality for Agriculture (Rome).
- Back, W., 1960. Origin of Hydrochemical Facies and Groundwater Flow Patterns in Northern Part of Atlantic Coastal Plain. International Geology Congress, pp. 87–95.
- Barth, S., 1993. Boron isotope variations in nature: a synthesis. Geol. Rundsch. 82, 640–651. https://doi.org/10.1007/BF00191491.
- Bentley, R.A., 2006. Strontium isotopes from the earth to the archaeological skeleton: a review. J. Archaeol. Method Theory 13, 135–187. https://doi.org/10.1007/s10816-006-9009-x.
- Bern, C.R., Boehlke, A.R., Engle, M.A., Geboy, N.J., Schroeder, K.T., Zupancic, J.W., 2013. Shallow groundwater and soil chemistry response to 3 years of subsurface drip irrigation using coalbed-methane-produced water. Hydrogeol. J. 21, 1803–1820. https://doi.org/10.1007/s10040-013-1058-0.
- Bern, C.R., Clark, M.L., Schmidt, T.S., Holloway, J.A.M., McDougal, R.R., 2015. Soil disturbance as a driver of increased stream salinity in a semiarid watershed undergoing energy development. J. Hydrol. 524, 123–136. https://doi.org/10.1016/j. ihydrol.2015.02.020.

- Blewett, T.A., Weinrauch, A.M., Delompré, P.L.M., Goss, G.G., 2017. The effect of hydraulic flowback and produced water on gill morphology, oxidative stress and antioxidant response in rainbow trout (Oncorhynchus mykiss). Sci. Rep. 7, 46582. https://doi. org/10.1038/srep46582.
- Blewett, T.A., Delompré, P.L.M., Glover, C.N., Goss, G.G., 2018. Physical immobility as a sensitive indicator of hydraulic fracturing fluid toxicity towards Daphnia magna. Sci. Total Environ. 635. 639–643. https://doi.org/10.1016/i.scitotenv.2018.04.165.
- Bouchaou, L., Michelot, J.L., Vengosh, A., Hsissou, Y., Qurtobi, M., Gaye, C.B., Bullen, T.D., Zuppi, G.M., 2008. Application of multiple isotopic and geochemical tracers for investigation of recharge, salinization, and residence time of water in the Souss-Massa aquifer, southwest of Morocco. J. Hydrol. 352, 267–287. https://doi.org/10.1016/j. ibvdrol.2008.01.022.
- Cammack, K.M., Wright, C.L., Austin, K.J., Johnson, P.S., Cockrum, R.R., Kessler, K.L., Olson, K.C., 2010. Effects of high-sulfur water and clinoptilolite on health and growth performance of steers fed forage-based diets. J. Anim. Sci. 88, 1777–1785. https://doi.org/10.2527/jas.2009-2343.
- Cañedo-Argüelles, M., Kefford, B.J., Piscart, C., Prat, N., Schäfer, R.B., Schulz, C.J., 2013. Salinisation of rivers: an urgent ecological issue. Environ. Pollut. 173, 157–167. https://doi.org/10.1016/j.envpol.2012.10.011.
- Chapman, E.C., Capo, R.C., Stewart, B.W., Kirby, C.S., Hammack, R.W., Schroeder, K.T., Edenborn, H.M., 2012. Geochemical and strontium isotope characterization of produced waters from marcellus shale natural gas extraction. Environ. Sci. Technol. 46, 3545–3553. https://doi.org/10.1021/es204005g.
- Chetelat, B., Gaillardet, J., 2005. Boron isotopes in the Seine River waters, France: a probe of anthropogenic contamination. Environ. Sci. Technol. 39, 2486–2493. https://doi. org/10.1021/es800725z.
- Clark, M.L., 2012. Water-quality Characteristics and Trend Analyses for the Tongue, Powder, Cheyenne, and Belle Fourche River Drainage Basins, Wyoming and Montana, for Selected Periods, Water Years 1991 Through 2010 (Reston, VA).
- Clark, M.L., Davidson, S.L., 2009. Specific Conductance and Dissolved-solids Characteristics for the Green River and Muddy Creek, Wyoming, Water Years 1999–2008 (Reston, VA). Clark, I., Fritz, P., 1997. Environmental Isotopes in Hydrogeology. Lewis Publishers, New York.
- Clark, C., Veil, J., 2015. U.S. Produced Water Volumes and Management Practices. Groundw. Prot. Counc., p. 119.
- Claypool, G.E., Holser, W.T., Kaplan, I.R., Sakai, H., Zak, I., 1980. The age curves of sulfur and oxygen isotopes in marine sulfate and their mutual interpretation. Chem. Geol. 28, 199–260. https://doi.org/10.1016/0009-2541(80)90047-9.
- Corsi, S.R., De Cicco, L.A., Lutz, M.A., Hirsch, R.M., 2015. River chloride trends in snow-affected urban watersheds: increasing concentrations outpace urban growth rate and are common among all seasons. Sci. Total Environ. https://doi.org/10.1016/j.scitotenv.2014.12.012.
- Cozzarelli, I.M., Skalak, K.J., Kent, D.B., Engle, M.A., Benthem, A., Mumford, A.C., Haase, K., Farag, A., Harper, D., Nagel, S.C., Iwanowicz, L.R., Orem, W.H., Akob, D.M., Jaeschke, J.B., Galloway, J., Kohler, M., Stoliker, D.L., Jolly, G.D., 2016. Environmental signatures and effects of an oil and gas wastewater spill in the Williston Basin, North Dakota. Sci. Total Environ. 579, 1781–1793. https://doi.org/10.1016/j.scitotenv.2016.11.157.
- Craig, H., 1961. Isotopic variations in meteoric waters. Science 133, 1702-1703.
- Daugherty, E.N., Ontiveros-Valencia, A.V., Rice, J.S., Wiest, M.J., Halden, R.U., 2010. Impact of point-of-use water softening on sustainable water reclamation: case study of the greater phoenix area. ACS Symp. Ser. 1048, 497–518. https://doi.org/10.1021/bk-2010-1048.ch025.
- Denison, R.E., Kirkland, D.W., Evans, R., 1998. Using strontium isotopes to determine the age and origin of gypsum and anhydrite beds. J. Geol. 106 (1).
- Dresel, P., Rose, A., 2010. Chemistry and origin of oil and gas well brines in western Pennsylvania. Pennsylvania Geol. Surv., 4th Ser. Open ..., p. 48 (doi:Open-File Report OFOG 1001.0).
- Dugan, H.A., Bartlett, S.L., Burke, S.M., Doubek, J.P., Krivak-Tetley, F.E., Skaff, N.K., Summers, J.C., Farrell, K.J., McCullough, I.M., Morales-Williams, A.M., Roberts, D.C., Ouyang, Z., Scordo, F., Hanson, P.C., Weathers, K.C., 2017. Salting our freshwater lakes. Proc. Natl. Acad. Sci. 114, 4453–4458. https://doi.org/10.1073/ pnas.1620211114.
- EPA, 2018. Study of oil and gas extraction wastewater management [WWW document].

  URL https://www.epa.gov/eg/study-oil-and-gas-extraction-wastewater-management.
- Fritz, S.J., 1994. A survey of charge-balance errors on published analyses of potable ground and surface waters. Groundwater 32, 539–546.
- Geeza, T.J., Gillikin, D.P., McDevitt, B., Van Sice, K., Warner, N.R., 2018. Accumulation of Marcellus formation oil and gas wastewater metals in freshwater mussel shells. Environ. Sci. Technol. 52, 10883–10892. https://doi.org/10.1021/acs.est.8b02727.
- Gould, D.H., McAllister, M.M., Savage, J.C., Hamar, D.W., 1991. High sulfide concentrations in rumen fluid associated with nutritionally induced polioencephalomalacia in calves. Am. J. Vet. Res. 52, 1164–1169.
- Guerra, K., Dahm, K., Dundorf, S., 2011. Oil and gas produced water management and beneficial use in the Western United States. Denver. doi. www.usbr.gov/pmts/water/publications/reports.html.
- Harkness, J.S., Darrah, T.H., Warner, N.R., Whyte, C.J., Moore, M.T., Millot, R., Kloppmann, W., Jackson, R.B., Vengosh, A., 2017. The geochemistry of naturally occurring methane and saline groundwater in an area of unconventional shale gas development. Geochim. Cosmochim. Acta 208, 302–334. https://doi.org/10.1016/j.gca.2017.03.039.
- Hindshaw, R.S., Tosca, R., Goût, T.L., Farnan, I., Tosca, N.J., Tipper, E.T., 2019. Experimental constraints on Li isotope fractionation during clay formation. Geochim. Cosmochim. Acta https://doi.org/10.1016/j.gca.2019.02.015.
- Hoffman, G.J., Maas, E.V., Prichard, T.L., Meyer, J.L., 1983. Salt tolerance of corn in the Sacramento-San Joaquin Delta of California. Irrig. Sci. 4, 31–44. https://doi.org/ 10.1007/BF00285555.

- Huh, Y., Chan, L.H., Zhang, L., Edmond, J.M., 1998. Lithium and its isotopes in major world rivers: implications for weathering and the oceanic budget. Geochim. Cosmochim. Acta https://doi.org/10.1016/S0016-7037(98)00126-4.
- James, K.R., Hart, B.T., Bailey, P.C.E., Blinn, D.W., 2009. Impact of secondary salinisation on freshwater ecosystems: effect of experimentally increased salinity on an intermittent floodplain wetland. Mar. Freshw. Res. 60, 246–258. https://doi.org/10.1071/ MF08099
- Jin, L., Siegel, D.I., Lautz, L.K., Mitchell, M.J., Dahms, D.E., Mayer, B., 2010. Calcite precipitation driven by the common ion effect during groundwater-surface-water mixing: a potentially common process in streams with geologic settings containing gypsum. Bull. Geol. Soc. Am. 122, 1027–1038. https://doi.org/10.1130/B30011.1.
- Kandylis, K., 1984. Toxicology of sulfur in ruminants: review. J. Dairy Sci. 67, 2179–2187. https://doi.org/10.3168/jds.S0022-0302(84)81564-7.
- Kaushal, S.S., 2016. Increased salinization decreases safe drinking water. Environ. Sci. Technol. 50, 2765–2766. https://doi.org/10.1021/acs.est.6b00679.
- Kaushal, S.S., Doody, T.R., Galella, J.G., Räike, A., Wessel, B., Jaworski, N., Kortelainen, P., Skinner, V., Morel, C., Likens, G.E., Haq, S., Wood, K.L., Pace, M.L., Utz, R., 2018a. Novel 'chemical cocktails' in inland waters are a consequence of the freshwater salinization syndrome. Philos. Trans. R. Soc. B Biol. Sci. 374. https://doi.org/10.1098/rsth.2018.0017
- Kaushal, S.S., Likens, G.E., Pace, M.L., Utz, R.M., Haq, S., Gorman, J., Grese, M., 2018b. Freshwater salinization syndrome on a continental scale. Proc. Natl. Acad. Sci. U. S. A. 115, E574–E583. https://doi.org/10.1073/pnas.1711234115.
- Kelly, V.R., Stack, W.P., Band, L.E., Belt, K.T., Fisher, G.T., Likens, G.E., Kaushal, S.S., Groffman, P.M., 2005. From the cover: increased salinization of fresh water in the northeastern United States. Proc. Natl. Acad. Sci. 102, 13517–13520. https://doi.org/ 10.1073/pnas.0506414102.
- Kendall, C., Coplen, T.B., 2001. Distribution of oxygen-18 and deuterium in river waters across the United States. Hydrol. Process. 15, 1363–1393. https://doi.org/10.1002/ hyp.217.
- Kondash, A.J., Lauer, N.E., Vengosh, A., 2018. The intensification of the water footprint of hydraulic fracturing. Sci. Adv. 4. https://doi.org/10.1126/sciadv.aar5982.
- Lauer, N.E., Harkness, J.S., Vengosh, A., 2016. Brine spills associated with unconventional oil development in North Dakota. Environ. Sci. Technol. https://doi.org/10.1021/acs. est.5b06349 acs.est.5b06349.
- Lgourna, Z., Warner, N., Bouchaou, L., Boutaleb, S., Hssaisoune, M., Tagma, T., Ettayfi, N., Vengosh, A., 2014. Elucidating the sources and mechanisms of groundwater salinization in the Ziz Basin of southeastern Morocco. Environ. Earth Sci. 73, 77–93. https:// doi.org/10.1007/s12665-014-3396-1.
- Lueth, V.W., Rye, R.O., Peters, L., 2005. "Sour gas" hydrothermal jarosite: ancient to modern acid-sulfate mineralization in the southern Rio Grande Rift. Chem. Geol. https://doi.org/10.1016/j.chemgeo.2004.06.042.
- Macpherson, G.L., Capo, R.C., Stewart, B.W., Phan, T.T., Schroeder, K., Hammack, R.W., 2014. Temperature-dependent Li isotope ratios in Appalachian Plateau and Gulf Coast Sedimentary Basin saline water. Geofluids 14, 419–429. https://doi.org/ 10.1111/cfl.12024
- Macpherson, G.L., Capo, R.C., Stewart, B.W., Phan, T.T., Schroeder, K., Hammack, R.W., 2014b. Temperature-dependent Li isotope ratios in Appalachian Plateau and Gulf Coast Sedimentary Basin saline water. Geofluids 14, 419–429. https://doi.org/ 10.1111/efl.12084.
- Marriott, C.S., Henderson, G.M., Crompton, R., Staubwasser, M., Shaw, S., 2004. Effect of mineralogy, salinity, and temperature on Li/Ca and Li isotope composition of calcium carbonate. Chem. Geol. https://doi.org/10.1016/j.chemgeo.2004.08.002.
- McDevitt, B., McLaughlin, M., Cravotta, C.A., Ajemigbitse, M.A., Sice, K.J.V., Blotevogel, J., Borch, T., Warner, N.R., 2018. Emerging investigator series: radium accumulation in carbonate river sediments at oil and gas produced water discharges: implications for beneficial use as disposal management. Environ. Sci. Process. Impacts https://doi.org/10.1039/c8em00336j.
- McLaughlin, M.C., Blotevogel, J., Watson, R.A., Schell, B., Blewett, T.A., Folkerts, E.J., Goss, G.G., Truong, L., Tanguay, R.L., Argueso, J.L., Borch, T., 2020a. Mutagenicity assessment downstream of oil and gas produced water discharges intended for agricultural beneficial reuse. Science of the Total Environment 715 (136944). https://doi.org/10.1016/j.scitotenv.2020.136944.
- McLaughlin, M.C., Borch, T., McDevitt, B., Warner, N.R., Blotevogel, J., 2020b. Water quality assessment downstream of oil and gas produced water discharges intended for beneficial reuse in arid regions. Sci. Total Environ. 713. https://doi.org/10.1016/j.scitotenv.2020.136607.
- Millot, R., Vigier, N., Gaillardet, J., 2010. Behaviour of lithium and its isotopes during weathering in the Mackenzie Basin, Canada. Geochim. Cosmochim. Acta https://doi. org/10.1016/j.gca.2010.04.025.
- Murphy, M.J., Porcelli, D., Pogge von Strandmann, P.A.E., Hirst, C.A., Kutscher, L., Katchinoff, J.A., Mörth, C.M., Maximov, T., Andersson, P.S., 2019. Tracing silicate weathering processes in the permafrost-dominated Lena River watershed using lithium isotopes. Geochim. Cosmochim. Acta 245, 154–171. https://doi.org/10.1016/j.gca.2018.10.024.
- NRCS, 2019. NRCS web soil survey [WWW document]. URL. https://websoilsurvey.sc.egov.usda.gov/App/HomePage.htm.
- Phan, T.T., Capo, R.C., Stewart, B.W., Macpherson, G.L., Rowan, E.L., Hammack, R.W., 2016. Factors controlling Li concentration and isotopic composition in formation waters and host rocks of Marcellus Shale, Appalachian Basin. Chem. Geol. https://doi.org/ 10.1016/j.chemgeo.2015.11.003.
- Pick, T., 2011. Assessing Water Quality for Human Consumption, Agriculture, and Aquatic

- Porowski, A., 2014. Isotope hydrogeology. Handbook of Engineering Hydrology: Fundamentals and Applications. https://doi.org/10.1201/b15625.
- Qi, H., Ma, C., He, Z., Hu, X., Gao, L., 2019. Lithium and its isotopes as tracers of groundwater salinization: a study in the southern coastal plain of Laizhou Bay, China. Sci. Total Environ. https://doi.org/10.1016/j.scitotenv.2018.09.122.
- Raisbeck, M., Riker, S., Tate, C., Jackson, R., Smith, M., Reddy, K., Zygmunt, J., 2008. Water Quality for Wyoming Livestock & Wildlife.
- Sedlacko, E.M., Jahn, C.E., Heuberger, A.L., Sindt, N.M., Miller, H.M., Borch, T., Blaine, A.C., Cath, T.Y., Higgins, C.P., 2019. Potential for beneficial reuse of oil-and-gas-derived produced water in agriculture: physiological and morphological responses in spring wheat (*Triticum aestivum*). Environ. Toxicol. Chem. https://doi.org/10.1002/etc.4449 etc.4449.
- Sharp, Z., 2007. Stable Isotope Geochemistry. Pearson Prentice Hall, Upper Saddle River. Stets, E.G., Lee, C.J., Lytle, D.A., Schock, M.R., 2018. Increasing chloride in rivers of the conterminous U.S. and linkages to potential corrosivity and lead action level exceedances in drinking water. Sci. Total Environ. https://doi.org/10.1016/j.scitotenv.2017.07.119.
- Szynkiewicz, A., Talon Newton, B., Timmons, S.S., Borrok, D.M., 2012. The sources and budget for dissolved sulfate in a fractured carbonate aquifer, southern Sacramento Mountains, New Mexico, USA. Appl. Geochem. https://doi.org/10.1016/j.apgeochem.2012.04.011.
- Szynkiewicz, A., Borrok, D.M., Skrzypek, G., Rearick, M.S., 2015. Isotopic studies of the Upper and Middle Rio Grande. Part 1 importance of sulfide weathering in the riverine sulfate budget. Chem. Geol. https://doi.org/10.1016/j.chemgeo.2015.05.022.
- Tasker, T.L., Burgos, W.D., Piotrowski, P., Castillo-Meza, L., Blewett, T.A., Ganow, K.B., Stallworth, A., Delompré, P.L.M., Goss, G.G., Fowler, L.B., Vanden Heuvel, J.P., Dorman, F., Warner, N.R., 2018. Environmental and human health impacts of spreading oil and gas wastewater on roads. Environ. Sci. Technol. https://doi.org/10.1021/acs.est.8b00716 acs.est.8b00716.
- Van Sice, K., Cravotta, C.A., McDevitt, B., Tasker, T.L., Landis, J.D., Puhr, J., Warner, N.R., 2018. Radium attenuation and mobilization in stream sediments following oil and gas wastewater disposal in western Pennsylvania. Appl. Geochem. 98. https://doi. org/10.1016/j.apgeochem.2018.10.011.
- Vengosh, A., 2013. Salinization and saline environments. Treatise on Geochemistry: Second Edition, 2nd ed Elsevier Ltd. https://doi.org/10.1016/B978-0-08-095975-7.00909-8.
- Vengosh, A., Jackson, R.B., Warner, N., Darrah, T.H., Kondash, A., 2014. A critical review of the risks to water resources from unconventional shale gas development and hydraulic fracturing in the United States. Environ. Sci. Technol. 48, 8334–8348. https://doi. org/10.1021/es405118y.
- Vigier, N., Decarreau, A., Millot, R., Carignan, J., Petit, S., France-Lanord, C., 2008. Quantifying Li isotope fractionation during smectite formation and implications for the Li cycle. Geochim. Cosmochim. Acta https://doi.org/10.1016/j.gca.2007.11.011.
- Vinson, D.S., Mcintosh, J.C., Dwyer, G.S., Vengosh, A., 2011. Arsenic and other oxyanion-forming trace elements in an alluvial basin aquifer: evaluating sources and mobilization by isotopic tracers (Sr, B, S, O, H, Ra). Appl. Geochem. https://doi.org/10.1016/j.apgeochem.2011.05.010.
- Vinson, D.S., Tagma, T., Bouchaou, L., Dwyer, G.S., Warner, N.R., Vengosh, A., 2013. Occurrence and mobilization of radium in fresh to saline coastal groundwater inferred from geochemical and isotopic tracers (Sr, S, O, H, Ra, Rn). Appl. Geochem. 38, 161–175. https://doi.org/10.1016/j.apgeochem.2013.09.004.
- Vredenburgh, L.D., Cheney, E.S., 1971. Sulfur and carbon isotopic investigation of petroleum, Wind River basin, Wyoming. Am. Assoc. Pet. Geol. Bull. 55, 1954–1975.
- Warner, N.R., Jackson, R.B., Darrah, T.H., Osborn, S.G., Down, A., Zhao, K., White, A., Vengosh, A., 2012. From the cover: geochemical evidence for possible natural migration of Marcellus formation brine to shallow aquifers in Pennsylvania. Proc. Natl. Acad. Sci. 109, 11961–11966. https://doi.org/10.1073/pnas.1121181109.
- Warner, N.R., Christie, C.A., Jackson, R.B., Vengosh, A., 2013a. Impacts of shale gas waste-water disposal on water quality in Western Pennsylvania. Environ. Sci. Technol. 47. https://doi.org/10.1021/es402165b.
- Warner, N.R., Lgourna, Z., Bouchaou, L., Boutaleb, S., Tagma, T., Hsaissoune, M., Vengosh, A., 2013b. Integration of geochemical and isotopic tracers for elucidating water sources and salinization of shallow aquifers in the sub-Saharan Drâa Basin, Morocco. Appl. Geochem. 34, 140–151. https://doi.org/10.1016/j.apgeochem.2013.03.005.
- Warner, N.R., Lgourna, Z., Bouchaou, L., Boutaleb, S., Tagma, T., Hsaissoune, M., Vengosh, A., 2013c. Applied geochemistry integration of geochemical and isotopic tracers for elucidating water sources and salinization of shallow aquifers in the sub-Saharan Drâa Basin, Morocco. Appl. Geochem. 34, 140–151. https://doi.org/10.1016/j.apgeochem.2013.03.005.
- Warner, N.R., Darrah, T.H., Jackson, R.B., Millot, R., Kloppmann, W., Vengosh, A., 2014. New tracers identify hydraulic fracturing fluids and accidental releases from oil and gas operations. Environ. Sci. Technol. 48, 12552–12560. https://doi.org/10.1021/ es5032135.
- Weber-Scannell, P.K., Duffy, L.K., 2007. Effects of total dissolved solids on aquatic organisms: a review of literature and recommendation for salmonid species. Am. J. Environ. Sci. https://doi.org/10.3844/aiessp.2007.1.6.
- Williams, W.D., 2001. Anthropogenic salinisation of inland waters. Hydrobiologia 466, 329–337. https://doi.org/10.1023/A:1014598509028.
- Wilson, J.M., Vanbriesen, J.M., 2012. Oil and gas produced water management and surface Pennsylvania. Environ. Pract. 14, 288–301.